

The unique $\alpha 4(+)/(-)\alpha 4$ agonist binding site in $(\alpha 4)_3(\beta 2)_2$ subtype nicotinic acetylcholine receptors permits differential agonist desensitization pharmacology vs. the $(\alpha 4)_2(\beta 2)_3$ subtype.

J. Brek Eaton[†], Linda M. Lucero[†], Harrison Stratton, Yongchang Chang, John F. Cooper, Jon.
M. Lindstrom, Ronald J. Lukas, and Paul Whiteaker

Division of Neurobiology, Barrow Neurological Institute, 350 West Thomas Road, Phoenix, AZ
85013 (J.B.E., L.M.L., H.S., Y.C., R.J.L., P.W.); Department of Neuroscience, Medical School of
the University of Pennsylvania, 217 Stemmler Hall, Philadelphia, PA 19104 (J.F.C., J.M.L.)

Running Title: HS vs. LS $\alpha 4\beta 2$ nicotinic receptor agonist desensitization.

Corresponding Author: Paul Whiteaker, Ph.D.

Laboratory of Neurochemistry

Division of Neurobiology

Barrow Neurological Institute

350 West Thomas Road

Phoenix, AZ 85013.

TEL: (602) 406 6534

FAX: (602) 406 4172

Email: paul.whiteaker@dignityhealth.org

Pages: 54 (including all figures, tables, and supplemental data)

Tables: 2

Figures: 9 (plus one supplemental figure)

References: 46

Abstract: 247

Introduction: 730

Discussion: 1784

Abbreviations: A-85380, 3-(2(S)-azetidylmethoxy)pyridine; ACh, acetylcholine; CRC, concentration response curve; HS, high-sensitivity; HSP, high-sensitivity pentameric concatemer; LS, low-sensitivity; LSP, low-sensitivity pentameric concatemer; nAChR, nicotinic acetylcholine receptor(s); Saz-A, 6-(5-(((S)-azetidin-2-yl)methoxy)pyridine-3-yl)hex-5-yn-1-ol (also known as AMOP-H-OH).

Recommend assignment to: Neuropharmacology section

ABSTRACT

Selected nicotinic agonists were used to activate and desensitize high-sensitivity (HS; $(\alpha 4)_2(\beta 2)_3$) or low-sensitivity (LS; $(\alpha 4)_3(\beta 2)_2$) isoforms of human $\alpha 4\beta 2$ -nicotinic acetylcholine receptors (nAChR). Function was assessed using $^{86}\text{Rb}^+$ efflux in a stably-transfected SH-EP1- $\alpha 4\beta 2$ human epithelial cell line, and two-electrode voltage-clamp electrophysiology in *Xenopus* oocytes expressing concatenated pentameric HS or LS $\alpha 4\beta 2$ -nAChR constructs (HSP and LSP). Unlike previously-studied agonists, desensitization by the highly-selective agonists A-85380 and sazetidine-A (Saz-A) preferentially reduced $\alpha 4\beta 2$ -nAChR HS-phase vs. LS-phase responses. The concatenated-nAChR experiments confirmed that $\approx 20\%$ of LS-isoform ACh-induced function occurs in an HS-like phase, which is abolished by Saz-A preincubation. Six mutant LSP were generated, each targeting a conserved agonist-binding residue within the LS-isoform-only $\alpha 4(+)/(-)\alpha 4$ interface agonist binding site. Every mutation reduced the percentage of LS-phase function, demonstrating that this site underpins LS-phase function. Oocyte-surface expression of the HSP and each of the LSP constructs was statistically indistinguishable, as measured using $\beta 2$ -subunit-specific [^{125}I]mAb295 labeling. However, maximum function is approximately 5x greater on a “per receptor” basis for unmodified-LSP vs. HSP $\alpha 4\beta 2$ -nAChR. Thus, recruitment of the $\alpha 4(+)/(-)\alpha 4$ site at higher agonist concentrations appears to augment otherwise-similar function mediated by the pair of $\alpha 4(+)/(-)\beta 2$ sites shared by both isoforms. These studies elucidate the receptor-level differences underlying the differential pharmacology of the two $\alpha 4\beta 2$ -nAChR isoforms, and demonstrate that HS vs. LS $\alpha 4\beta 2$ -nAChR activity can be selectively manipulated using pharmacological approaches. Since $\alpha 4\beta 2$ nAChR are the predominant neuronal subtype these discoveries likely have significant functional implications, and may provide important insights for drug discovery and development.

Nicotinic acetylcholine receptors (nAChR) are prototypical members of the ligand-gated ion channel superfamily of neurotransmitter receptors. Vertebrate nAChR exist as a diverse family of subtypes defined by their compositions as pentamers of homologous subunits derived from at least seventeen genes ($\alpha 1$ - $\alpha 10$, $\beta 1$ - $\beta 4$, γ , δ , ϵ). Each nAChR subtype has characteristic pharmacological and biophysical properties that, nevertheless, can overlap with those of other subtypes (Gotti et al., 2009).

The predominant nAChR subtype in the brain, with high binding affinity for nicotine and other agonists, contains $\alpha 4$ and $\beta 2$ subunits ($\alpha 4\beta 2$ -nAChR; (Flores et al., 1992; Whiting and Lindstrom, 1987)). $\alpha 4\beta 2$ -nAChR have been implicated in perception, cognition, and emotion; in nicotine self-administration, reward, and dependence; and in diseases such as Alzheimer's and epilepsy (Cordero-Erausquin et al., 2000; Lindstrom, 2003; Picciotto et al., 1995; Steinlein, 2001). Initial evidence based on site-directed mutagenesis and immunochemical studies of heterologously-expressed receptors indicated that $\alpha 4\beta 2$ -nAChR have an $(\alpha 4)_2(\beta 2)_3$ subunit stoichiometry (Anand et al., 1991; Cooper et al., 1991). However later heterologous expression studies using *Xenopus* oocytes showed that, when ratios of expressed nAChR $\alpha 4$ and $\beta 2$ subunits were manipulated, it was possible to produce two $\alpha 4\beta 2$ -nAChR isoforms. When $\beta 2$ subunit cRNA is present in ≈ 10 -fold excess over $\alpha 4$ subunit cRNA, an isoform with high sensitivity (HS) to activation by agonists and a presumed $(\alpha 4)_2(\beta 2)_3$ stoichiometry is produced. In oocytes injected with the opposite subunit ratio ($\approx 10:1$ of $\alpha 4:\beta 2$ subunit cRNAs), an isoform with lower agonist sensitivity (LS) predominates, with a presumed $(\alpha 4)_3(\beta 2)_2$ stoichiometry (Zwart and Vijverberg, 1998). Related work in transfected cell lines reinforced the findings in oocytes (Nelson et al., 2003). Further, agonist concentration-response curve (CRC) analyses in wild-type mice are consistent with the idea that a mixture of HS and LS $\alpha 4\beta 2$ -nAChR isoforms is naturally expressed (Marks et al., 1999). Functional assessments in heterozygotic nAChR $\alpha 4$ - or $\beta 2$ -subunit-null mutant mice (which therefore express a biased ratio of these genes compared

to wild-type mice) are consistent with of the concept that native HS and LS $\alpha 4\beta 2$ -nAChR isoforms also have $\alpha 4:\beta 2$ subunit ratios of 2:3 and 3:2, respectively (Gotti et al., 2008). Work using linked-subunit (concatemeric) constructs allowed the expression of $\alpha 4\beta 2$ -nAChR with completely defined subunit compositions, and confirmed these putative stoichiometries (Carbone et al., 2009; Zhou et al., 2003). Recent studies show that $(\alpha 4)_2(\beta 2)_3$ and $(\alpha 4)_3(\beta 2)_2$ share the same pair of conserved, long-recognized, agonist binding sites present at the interfaces between the primary (+) face of the $\alpha 4$ subunit and the complementary (-) face of the $\beta 2$ subunit (i.e. at $\alpha 4(+)/(-)\beta 2$ interfaces). However, an additional binding site is located at the $\alpha 4(+)/(-)\alpha 4$ interface found only in LS $\alpha 4\beta 2$ -nAChR. Site-directed mutagenesis and covalent modification experiments demonstrate that the $\alpha 4(+)/(-)\alpha 4$ site is required for effective activation of $(\alpha 4)_3(\beta 2)_2$ -nAChR, giving rise to their distinctive LS pharmacology (Harpsøe et al., 2011; Mazzaferro et al., 2011).

HS and LS $\alpha 4\beta 2$ -nAChR isoforms have different sensitivities to the antagonists methyllycaconitine and dihydro- β -erythroidine (Marks et al., 1999), but concentrations at which agonists such as epibatidine, nicotine, cytosine and methylcarbachol induce desensitization are not different between HS and LS $\alpha 4\beta 2$ -nAChR (Marks et al., 2010). However, none of these agonists is especially selective between activation of HS and LS nAChR (Marks et al., 1999) or thus, presumably, between $\alpha 4(+)/(-)\beta 2$ and $\alpha 4(+)/(-)\alpha 4$ agonist binding sites. In this study, we sought to use more discriminating ligands to dissect the roles played by $\alpha 4(+)/(-)\beta 2$ and $\alpha 4(+)/(-)\alpha 4$ interfaces in HS and/or LS $\alpha 4\beta 2$ -nAChR isoforms. We investigated activation and desensitization of receptors in response to ACh and to two, highly HS- vs LS-selective, nicotinic agonists that might better discriminate between $\alpha 4\beta 2$ -nAChR isoforms, A-85380 (Abreo et al., 1996) [3-(2(S)-azetidylmethoxy)pyridine] and sazetidine-A (Xiao et al., 2006) [6-(5-(((S)-azetidin-2-yl)methoxy)pyridine-3-yl)hex-5-yn-1-ol; henceforth abbreviated as Saz-A]. We report that HS-phase $\alpha 4\beta 2$ -nAChR responses can be selectively inactivated by low concentrations of

either ligand, while leaving LS-phase responses in a state that can still be activated by acute agonist application. We also show that single residue mutations targeted to $\alpha 4(+)/(-)\alpha 4$ interfaces can affect i) functional activity, ii) the balance of HS- vs LS-phase activation, and iii) agonist sensitivity of $(\alpha 4)_3(\beta 2)_2$ -nAChR, further demonstrating the functional significance of this recently-recognized site. These findings, especially when coupled with the realization that different $\alpha 4\beta 2$ -nAChR isoforms will respond differently to endogenous concentrations of ACh and the presence of exogenous nicotinic agonists, suggest novel drug discovery and development opportunities for $\alpha 4\beta 2$ -AChR. These possibilities may also apply to other members of the LGIC superfamily that also contain ligand-binding subunit interfaces related to the recently-discovered $\alpha 4/\alpha 4$ site.

MATERIALS AND METHODS

Chemicals other than those kindly provided by Drs. Alan Kozikowski (University of Illinois, Chicago, IL) or F. Ivy Carroll (Research Triangle Institute, Research Triangle Park, NC) were sourced from Sigma-Aldrich Co. LLC (St. Louis, MO) unless specified otherwise.

Cell culture:

Cells of the SH-EP1 human epithelial cell line were kindly provided by Dr. June Biedler, Sloan-Kettering Institute for Cancer Research (New York, NY). SH-EP1-h α 4 β 2 cells [stably transfected SH-EP1 epithelial cells heterologously expressing human α 4 β 2-nAChR (Eaton et al., 2003)] were grown in DMEM (high glucose, bicarbonate-buffered, with 1 mM sodium pyruvate and 8 mM L-glutamine) supplemented with 100 U/ml penicillin and 100 μ g/ml streptomycin (all from MediaTech, Inc., Manassas, VA) plus 10% horse serum (Life Technologies, Inc., Gaithersburg, MD) and 5% fetal bovine serum (Atlanta Biologicals, Atlanta, GA) on 100-mm diameter tissue culture plates in a humidified atmosphere containing 5% CO₂ in air at 37 °C (Eaton et al., 2003). Positive selection for expression of the α 4 and β 2 subunits (in pcDNA3.1/Zeo and pcDNA3.1/Hygro, respectively; Invitrogen, Carlsbad, CA) was maintained by further supplementation of the growth medium with 0.25 mg/ml zeocin (Invitrogen) and 0.4 mg/ml hygromycin B (Calbiochem, San Diego, CA).

Cell-line nAChR functional assays (⁸⁶Rb⁺ efflux):

Function of α 4 β 2-nAChR expressed by human SH-EP1-h α 4 β 2 cells was determined using ⁸⁶Rb⁺ efflux assays (Lukas and Cullen, 1988). Cells were harvested at confluence from 100-mm plates by trypsinization (MediaTech, Inc., Manassas, VA) before being resuspended in complete medium and evenly seeded at a density of 1.5 confluent 100-mm dishes per 24-well plate (BD Falcon, Franklin Lakes, NJ). After cells had adhered (generally overnight, but no sooner than 4 hr later), medium was removed and replaced with 250 μ l per well of complete medium supplemented with ~300,000 cpm of ⁸⁶Rb⁺ (PerkinElmer, Waltham, MA), counted at 40% efficiency using

Cherenkov counting and a Packard TriCarb 1900 Liquid Scintillation Analyzer (PerkinElmer). After $^{86}\text{Rb}^+$ loading for at least 4 hr (typically overnight), $^{86}\text{Rb}^+$ efflux was measured using the “flip-plate” technique (Gentry et al., 2003), first employed to remove extracellular isotope by a rinse in efflux buffer (130 mM NaCl, 5.4 mM KCl, 2 mM CaCl_2 , 5 mM glucose, 50 mM HEPES, pH 7.4; all at room temperature) followed by a 10 min “preincubation” in a low, desensitizing concentration of agonist or in efflux buffer alone. Cells were then incubated for 5 min in the presence of ligands of choice at a range of concentrations in efflux buffer to define acute effects of drugs. Maximum efflux was defined in the presence of a maximally efficacious concentration of a full agonist (1 mM carbamylcholine; carbachol, which has been shown to be a full agonist in this assay (Eaton et al., 2003)), and non-specific ion flux was defined either in the absence of agonist or in the presence of agonist (1 mM carbamylcholine) plus antagonist at a maximally effective inhibitory concentration (100 μM mecamylamine). Specific ion flux in test samples was calculated as the increase over non-specific efflux and normalized as a percentage of specific efflux evoked by 1 mM carbamylcholine. Moreover, because some isotopic ion efflux occurred during the preincubation / desensitization period, not all cells retained the same amount of $^{86}\text{Rb}^+$ by the time that the assay for acute drug action was initiated. Accordingly, specific ion flux was further normalized as a percentage of intracellular $^{86}\text{Rb}^+$ present at the beginning of the agonist-induced efflux period. There was no recovery time between the preincubation and agonist-induced efflux periods.

Concatemeric HS and LS $\alpha 4\beta 2$ constructs:

Human, fully pentameric $(\alpha 4)_2(\beta 2)_3$ (HS isoform; $\beta 2\text{-}\alpha 4\text{-}\beta 2\text{-}\alpha 4\text{-}\beta 2$ subunit order) and $(\alpha 4)_3(\beta 2)_2$ (LS isoform; $\beta 2\text{-}\alpha 4\text{-}\beta 2\text{-}\alpha 4\text{-}\alpha 4$ subunit order) concatemeric nAChR constructs were provided in the pCI oocyte expression vector by Isabel Bermudez (Oxford Brookes; Oxford, U.K.). These HS pentamer (HSP) and LS pentamer (LSP) constructs were as previously described (Carbone et al., 2009), except that each of the original native $\beta 2$ subunit cDNA sequences were replaced with sequences optimized for expression in vertebrate expression

systems (synthesized by GeneArt, Life Technologies; Grand Island, NY). The replacement $\beta 2$ cDNA sequence encodes the native amino-acid sequence, but it is optimized by minimization of high-GC content sequence segments, improved codon usage, reduction of predicted RNA secondary structure formation, and removal of sequence repeats and possible alternative start and splice sites.

As described previously (Carbone et al., 2009), the linkers between each subunit in the HSP and LSP cDNA constructs contain unique restriction sites that allow removal and replacement of individual subunits (see Fig. 1). As previously demonstrated, the initial $\beta 2$ - $\alpha 4$ subunit protein pair of the LSP construct will assemble to form an orthosteric binding site between the complementary (-) face of the initial $\beta 2$ subunit and the principal (+) face of the following $\alpha 4$ subunit (Zhou et al., 2003). Accordingly, the assembled LSP (and HSP) $\alpha 4\beta 2$ -nAChR proteins host orthosteric agonist binding pockets at the $\alpha 4(+)/(-)\beta 2$ interfaces between the first and second, and the third and fourth, subunits. The recently-discovered, LS-only $\alpha 4(+)/(-)\alpha 4$ interface thus forms between the (-) face of the $\alpha 4$ subunit in LSP position four, and the (+) face of $\alpha 4$ subunit in position five (Harpsøe et al., 2011; Mazzaferro et al., 2011).

Canonical agonist binding pockets are predominantly formed from conserved residues from a set of three loops contributed by the (+) face of one α subunit (loops A-C), and by an additional loop contributed by the (-) face of the neighboring subunit (loop D, with smaller contributions from two further Loops; E & F (Brejc et al., 2002; Celie et al., 2004; Corringer et al., 2000; Xiu et al., 2009)). To assess the functional effects of mutating putative binding-pocket residues at the $\alpha 4(+)/(-)\alpha 4$ interface only present in the LSP construct (see Fig. 1), a set of six subunit mutants were synthesized (GeneArt, Life Technologies; Grand Island, NY). Mutation of a set of conserved aromatic amino acids (tyrosines and tryptophans; to alanine in each case) in Loops A-D was chosen (see Supplemental Figure 1). Mutations in Loops A-C were mapped to the (+)-face of the $\alpha 4$ subunit in LSP position 5, while the Loop D mutant mapped to the (-)-face

of the $\alpha 4$ subunit in LSP position 4 (Fig. 1). Each mutant subunit hosted one of the site-directed mutations together with the correct linker sequences and restriction sites to allow substitution for the target wild-type subunit within the LSP construct. Each aromatic residue that was mutated has been shown, by affinity labeling, X-ray crystallography, and / or site directed mutagenesis, to have significant interactions with bound agonists at canonical nAChR agonist binding sites (Brejc et al., 2002; Celie et al., 2004; Corringer et al., 2000; Xiu et al., 2009). Signal peptides were removed and replaced by linker peptides for all but the first subunit in each concatemer, but we use the conventional amino acid numbering scheme, starting with the translational initiation methionine as residue 1, and thus made the following mutations, all in the $\alpha 4$ subunit: W88A (loop D), Y126A (loop A), W182A & Y184 (loop B), and Y223 & Y230 (loop C; Fig. 2). For further context, the mutated $\alpha 4(+)$ face residues correspond to *Torpedo* $\alpha 1$ subunit conserved residues Y93 (loop A), W149 & Y151 (loop B), Y190 and Y198 (loop C), while the $\alpha 4(-)$ mutation was performed at the residue corresponding to the conserved W55 or W57 of loop D in *Torpedo* γ or δ subunits, respectively.

The mutant subunits were then substituted for the corresponding-position wild-type subunits. Wild-type LSP in the pCI oocyte expression vector was restriction enzyme digested to remove the target subunit (XhoI and NotI for $\alpha 4$ position 4, NotI and EcoRV for position 5; 2 h at 37 °C), the host construct was gel-purified, and the mutant subunit was ligated into the host. Correct substitution was confirmed using restriction digestion and by sequencing of the newly-incorporated mutant $\alpha 4$ subunits.

Concatemer RNA preparation for oocyte injection:

After plasmids were linearized with Swal (2 hrs at 37 °C), treated with proteinase K (30 minutes at 50 °C), and purified using Qiagen's PCR Clean-up Kit (Valencia, CA), cRNAs were transcribed using mMessage mMachine T7 kit (Applied Biosystems/Ambion, Austin, TX, USA). Reactions were treated with TURBO DNase (1U for 15 minutes at 37°C) and cRNAs were

purified using Qiagen RNeasy Clean-up kit (Valencia, CA). cRNAs were confirmed on a 1% agarose gel and stored at -80 °C.

Oocyte preparation and RNA injection:

Methods of oocyte isolation and processing for receptor expression have previously been described (Chang et al., 2002) but were modified as follows. *Xenopus* oocytes were purchased from Ecocyte LLC (Austin, TX) and were maintained at 13°C. The tips of pulled glass micropipettes were broken to achieve an outer diameter of ~40 µm (resistance of 2-6 MΩ), and pipettes were used to inject 80 nl containing 40 ng of RNA.

Two-electrode voltage-clamp (TEVC) determination of concatemeric construct functional expression in *Xenopus* oocytes:

8 d after injection, oocytes expressing nAChR subunits were voltage clamped at -70 mV with an Axoclamp 900A amplifier (Molecular Devices, Sunnyvale, CA, USA). Recordings were sampled at 10 kHz (low-pass Bessel filter: 40Hz; high-pass filter: DC), and the resulting traces were saved to disk (Molecular Devices Clampex v10.2), then extracted and analyzed using Clampfit software (Molecular Devices, Sunnyvale, CA). Data from oocytes with leak currents (I_{leak}) > 50 nA were excluded from recordings. Drugs were applied using a sixteen channel, gravity-fed, perfusion system with automated valve control (AutoMate Scientific, Inc.; Berkeley, CA), in oocyte Ringer's buffer (NaCl 82.5 mM, KCl 2.5 mM, MgCl₂ 1 mM, CaCl₂ 1 mM, Na₂HPO₄ 1 mM, HEPES 5 mM, supplemented with atropine sulfate 1.5 µM to block any possible muscarinic responses; pH = 7.5; OR2 buffer; flow rate = 4 mL min⁻¹). Post-valve tubing lengths were minimized, and a custom manifold was used to reduce dead volume, in order to optimize solution exchange at the oocyte (within the limitations imposed by the large size of a *Xenopus* oocyte). Typical valve openings were for 1 s (referred to henceforth as "1 s applications"). To obtain a practical measure of agonist pulse lengths as seen at the oocyte, 10 mM K⁺ pulses (K⁺ substituted for an equivalent amount of Na⁺ in OR2 buffer) were applied directly to the oocyte.

The resulting changes in membrane current under TEVC mode provided a receptor-independent measure of solution/oocyte contact time. Total application times following a 1s valve opening were measured as 1.45 ± 0.04 s (measured from the beginning to the end of the deflection from baseline current), and peak application was 0.80 ± 0.02 s (measuring the time the response plateau was ≥ 90 % of full K^+ -induced deflection). Values in each case are mean \pm SEM from four oocytes. In the case of A-85380 and Saz-A agonist acute application CRC experiments, the extremely low concentrations needed to define the lower part of the curve resulted in very slow response kinetics (presumably because of slow, diffusion rate limited, association of the agonist with the receptor). For agonist concentrations ≤ 10 nM, valve-open times were extended to 25 s in order to allow a full-peak response to develop.

[¹²⁵I]mAb295 labeling of Xenopus oocyte surface LSP nAChR populations:

Mutations at the LSP construct $\alpha 4/\alpha 4$ interface could potentially contribute to changed functional expression by altering cell-surface expression levels. To determine if this was the case, cell-surface nAChR expression levels were measured using [¹²⁵I]mAb295 binding assays. mAb295 is a monoclonal antibody raised against immunopurified chicken-brain nAChR, and has been demonstrated to recognize specifically human, bovine, and rodent nAChR $\beta 2$ subunits in native form (Lai et al., 2005; Whiteaker et al., 2006; Whiting and Lindstrom, 1988). Function of unmodified HSP & LSP, or variant LSP, constructs was first measured for individual oocytes, stimulated with a maximally-effective ACh concentration (100 μ M for HSP, 1 mM for LSP), using two-electrode voltage-clamp electrophysiology (see preceding description). $\beta 2$ -subunit specific [¹²⁵I]mAb295 was then used essentially as described previously (Kuryatov and Lindstrom, 2011) to measure nAChR expression on the surface of the same oocytes. Oocytes were incubated for 3 h in OR2 buffer supplemented with heat-inactivated normal horse serum (10%; to reduce non-specific binding) and 2 nM $\beta 2$ -specific [¹²⁵I]mAb295 (a saturating concentration (Whiteaker et al., 2009)). Unbound and non-specifically bound [¹²⁵I]mAb295 was removed by three washes

with ice-cold OR2 buffer (2 min each). Residual non-specific binding was determined by incubating non-injected oocytes in the same assay, and subtracted to calculate specific binding. Specific cell-surface binding of [125 I]mAb295 was converted to nAChR surface expression using the specific activity of the radiolabeled antibody and assuming two binding sites (i.e. β 2 subunits) per LSP nAChR, and three sites per HSP nAChR. The resulting nAChR expression data were then used to normalize concatemeric nAChR function.

Data Analysis:

Maximum function (E_{\max} for $^{86}\text{Rb}^+$ efflux, I_{\max} for two-electrode voltage clamp) and $\log EC_{50}$ / IC_{50} values were determined from individual concentration-response experiments by non-linear least-squares curve fitting (PRISM 5.0, GraphPad Software, Inc., La Jolla, CA). Unconstrained, monophasic or biphasic logistic equations were used to fit all parameters, including Hill slopes and fractional contributions of function attributable to HS or LS receptors, where applicable. Data were analyzed using Student's unpaired t-test (two-tailed) to compare pairs of groups, or by one-way or two-way ANOVA and Dunnett's multiple comparison test, in order to compare the means of three or more groups (GraphPad PRISM V5.0).

Homology modeling and ACh docking

The amino-terminal domain of the human α 4 nAChR subunit was aligned to the α 7 nAChR chimera sequence from the crystal structure of 3SQ6, with extra residues at the sequence ends trimmed. The homology models of two α 4 nAChR subunits were then built using ICM Pro 3.7 (Molsoft, San Diego, CA) with 3D templates of Chains A and B from the structure of 3SQ6. The resulting models were merged and optimized by ICM Pro. Docking of acetylcholine into the interface binding site of the homology model was performed with ICM Pro. The docked result was presented with Discovery Studio Visualizer 3.0 (Accelrys, San Diego, CA).

RESULTS

Acute agonist treatment in SH-EP1-h α 4 β 2 cells:

We studied the properties of two nicotinic agonists that have previously demonstrated unusually high degrees of selectivity between HS and LS α 4 β 2-nAChR: A-85380 and its derivative, Saz-A.

In SH-EP1-h α 4 β 2 cells, acute exposure to Saz-A produced a potent, concentration-dependent ($\log EC_{50} = -8.70 \pm 0.07$, $n_H = 1.9 \pm 0.4$), monophasic, and apparently partial agonist response (E_{max} $55 \pm 0.8\%$ of the carbachol control in this set of experiments; Fig. 2A). Notably, the Saz-A concentration-response profile plateaus over at least four orders of magnitude. This contrasts with some agonists with efficacy that is likely limited by self-inhibition at higher drug concentrations and which yield bell-shaped CRCs.

By contrast to the monophasic, apparent partial, agonist activity shown by Saz-A, acute exposure to A-85380 produced a strongly biphasic CRC. Peak efficacy was comparable ($108 \pm 10\%$) to that of carbachol, the full-agonist control. Approximately $31 \pm 18\%$ or $69 \pm 18\%$ of function was seen in the HS and LS phases, respectively, in this set of experiments. Log EC_{50} values were -8.40 ± 0.14 and -6.44 ± 0.25 , and n_H was 2.2 ± 1.6 and 0.7 ± 0.3 at the HS and LS isoforms, respectively (Fig. 2B). Note that curve fitting to five variables is inevitably subject to larger standard errors than for simpler concentration-response relationships.

Selective desensitization of HS-phase α 4 β 2-nAChR function in SH-EP1-h α 4 β 2 cells:

We next defined the effects of 10 min pretreatments with Saz-A or A-85380 on functional responses in SH-EP1-h α 4 β 2 cells subsequently subjected to acute agonist challenge. On the basis of the acute stimulation results (Figs. 3A-B), pretreatment was performed using 3.16 nM ($10^{-8.5}$ M) Saz-A or A-85380. This concentration was determined in pilot studies to be sufficiently low as to produce submaximal activation of HS-phase α 4 β 2-nAChR function without activating LS-phase α 4 β 2-nAChR responses (in the case of A-85380). Concentration-response

relationships were then defined for a 5 min acute challenge with agonist, which was co-applied with the drug used in the pretreatment, without a recovery period.

Acute responses to Saz-A were essentially abolished after a 10 min pretreatment with 3.16 nM Saz-A or 3.16 nM A-85380 (Fig. 2C). There was a small, but measurable amount of $^{86}\text{Rb}^+$ efflux ($\leq 10\%$ of that for the full-agonist carbamylcholine control) in samples pretreated with 3.16 nM Saz-A or A-85380. This background level of function was due to steady-state efflux elicited by undissociated ligand bound during the pretreatment, and it was indistinguishable from the level of function observed in control experiments where 3.16 nM drug pretreatments were followed by a treatment with buffer alone (data not shown, but this background level of function is evident from data at the lowest concentrations of drug used for acute challenge).

High concentrations of acutely applied A-85380 elicited functional responses from $\alpha 4\beta 2$ -nAChR in cells pretreated with the same 3.16 nM concentration of either Saz-A or A-85380 (Fig. 2D) that eliminated Saz-A-stimulated function. This is in strong contrast to the desensitization-induced full blockade of acute responses to Saz-A following the same pretreatment regime. After Saz-A or A-85380 pretreatment, the remaining response to acutely-applied high A-85380 concentrations closely resembled the LS $\alpha 4\beta 2$ -nAChR component of function that was evoked by acute application of higher concentrations of A-85380 in non-pretreated cells. After pretreatment with 3.16 nM A-85380, the response to acute A-85380 was monophasic, having a $\log\text{EC}_{50}$ value of -5.82 ± 0.04 , a Hill slope of 1.1 ± 0.1 , and efficacy of $80 \pm 2\%$. After pretreatment with 3.16 nM Saz-A, acute exposure to A-85380 elicited function with an EC_{50} value of -5.68 ± 0.04 , a Hill slope of 1.2 ± 0.2 , and efficacy of $72 \pm 2\%$. Taking into account the $\sim 10\%$ background response during the 3.16 nM pretreatments, this indicates that a concentration of Saz-A (3.16 nM) that abolished HS-phase function reduced LS-phase function from 69 % to 62 % of control, a reduction of only 11%. The A-85380 pretreatment effect on A-85380-induced LS-phase function was even less pronounced. In neither case was evidence seen of HS $\alpha 4\beta 2$ -

nAChR-mediated responses superimposed above the previously noted background response (Fig. 2D). Thus, it appears that the same pre-applied concentrations of Saz-A and A-85380 that strongly reduce HS-phase responses to either drug have little effect on LS-phase responses in the same cell line during 5 min stimulation, as measured when using $^{86}\text{Rb}^+$ efflux.

Acute Saz-A and A-85380 responses of HSP vs. LSP $\alpha 4\beta 2$ -nAChR expressed in *Xenopus* oocytes :

The results obtained in SH-EP1-h $\alpha 4\beta 2$ cells strongly suggested that pretreatment with Saz-A or A-85380 concentrations that greatly diminish HS-phase $\alpha 4\beta 2$ -nAChR responses may induce significantly less loss of LS-phase $\alpha 4\beta 2$ -nAChR function. We hypothesized that this was due to the recently-discovered existence of a third binding site of lower affinity, at the $\alpha 4(+)/(-)\alpha 4$ interface (Harpsoe et al., 2011; Mazzaferro et al., 2011). However, attempting to disentangle effects in the SH-EP1-h $\alpha 4\beta 2$ cells' mixed HS and LS $\alpha 4\beta 2$ -nAChR population could lead to errors of interpretation. In order to unequivocally study pure populations of HS or LS $\alpha 4\beta 2$ -nAChR, concatemeric constructs expressing functional $(\alpha 4)_2(\beta 2)_3$ and $(\alpha 4)_3(\beta 2)_2$ pentameric constructs (HSP and LSP, respectively; see Fig. 1) were employed. We first subjected these populations to acute Saz-A and A-85380 stimulation, to test whether similar responses could be identified between the cell-line- and oocyte-based expression models. This was indeed the case. As illustrated in Fig 3A, Saz-A produced a fully-efficacious (99 ± 2 % of ACh control) and highly-potent agonism ($\log\text{EC}_{50} = -8.53 \pm 0.06$) of HSP $\alpha 4\beta 2$ -nAChR. In contrast, Saz-A efficacy at LSP $\alpha 4\beta 2$ -nAChR was only 12 ± 2 % of ACh control, although a very similar potency was observed at both $\alpha 4\beta 2$ -nAChR isoforms (LSP $\log\text{EC}_{50} = -8.34 \pm 0.10$). Both CRCs were compatible with a single-site model, and produced similar Hill slopes (HSP Saz-A $n_H = 1.09 \pm 0.15$, LSP Saz-A $n_H = 1.02 \pm 0.23$). Acute A-85380 stimulation results were also compatible with the data obtained from the SH-EP1-h $\alpha 4\beta 2$ cell line, as shown in Fig 3B. Although a small HS-phase response may be visible in the A-85380 activation trace, this could not reliably be fit using a two-site model.

Because of this data were fit to a single-site model, which calculated similar Hill slopes for each CRC (HSP A-85380 $n_H = 1.10 \pm 0.12$, LSP A-85380 $n_H = 0.93 \pm 0.11$). A-85380 was highly efficacious at both $\alpha 4\beta 2$ -nAChR isoforms (115 ± 2 % efficacy compared to ACh control at HSP, 101 ± 3 % at LSP), but ≈ 200 -fold more potent at HSP vs. LSP nAChR (HSP $\log EC_{50} = -8.55 \pm 0.05$, LSP $\log EC_{50} = -6.27 \pm 0.06$).

Differential post-desensitization responses of HSP vs. LSP $\alpha 4\beta 2$ -nAChR concatemers expressed in *Xenopus* oocytes:

For this and subsequent preincubation experiments, Saz-A was chosen since it has a simpler agonist profile (producing very little activation of LS-phase function, unlike A-85380; see preceding section). Preincubation with 3.16 nM Saz-A reduced HSP $\alpha 4\beta 2$ I_{max} nAChR responses following acute exposure to a maximally-effective ACh dose to 17.6 ± 2.1 % of the control, no Saz-A preincubation response (Fig. 4). In contrast, 33.3 ± 3.0 % LSP $\alpha 4\beta 2$ -nAChR I_{max} function was retained under the same Saz-A (3.16 nM) preincubation conditions (Fig. 4). This difference was significant ($p < 0.01$; see legend of Fig. 4).

The oocyte Saz-A desensitization experiments require repeated stimulation of the same oocyte with ACh (30 μ M for HSP, 1 mM for LSP). ACh was chosen for these experiments because it is permanently charged, hydrophilic, and therefore easy to wash out of the test chamber. However, despite the 5 min wash period between control and test stimulations, it was possible that test responses could be blunted by preceding control stimulations. This possibility was tested by washing with buffer alone, rather than buffer plus Saz-A, between ACh stimulations. In the absence of Saz-A, HSP $\alpha 4\beta 2$ -nAChR test ACh responses were not reduced compared to preceding control responses (test response = 124 ± 13 % of control; data not shown). The same outcome was found with responses recorded from LSP $\alpha 4\beta 2$ -nAChR (test response = 109 ± 15 % of control; data not shown). Thus, the loss in agonist response observed following Saz-A

pretreatment was due only to Saz-A actions, and not to desensitization induced by the initial control ACh stimulations employed.

The $\alpha 4(+)/(-)\alpha 4$ subunit interface forms an agonist binding site that is required for effective LSP $\alpha 4\beta 2$ -nAChR activation by acute ACh stimulation:

HSP and LSP $\alpha 4\beta 2$ -nAChR share a pair of long-recognized agonist binding pockets, formed at the $\alpha 4(+)/(-)\beta 2$ subunit interfaces common to both $\alpha 4\beta 2$ isoforms (see Fig. 1). The ability of LS $\alpha 4\beta 2$ -nAChR to be stimulated by high agonist concentrations, even when the $\alpha 4(+)/(-)\beta 2$ sites are saturated (as demonstrated by loss of HSP responses), suggested that residual LS $\alpha 4\beta 2$ -nAChR function might be activated by agonist binding to the $\alpha 4(+)/(-)\alpha 4$ subunit interface only found in the LS isoform (see Materials and Methods section and Fig. 1). If so, mutation of critical residues within the $\alpha 4(+)/(-)\alpha 4$ site might be expected to reduce the relative amount of LS to HS function produced by $\alpha 4\beta 2$ LSP nAChR and / or to reduce the agonist potency for the LS phase of function. To test this hypothesis, a series of site-directed mutations were made to the $\alpha 4(+)/(-)\alpha 4$ subunit interface of the LSP construct. These mutations targeted highly-conserved aromatic residues known to be involved in agonist binding across multiple nAChR subtypes (see Methods, and Supplemental Figure 1).

When an un-mutated LSP $\alpha 4\beta 2$ -nAChR population was acutely stimulated with ACh, 21 ± 3 % of ACh-induced function fell into a “high-sensitivity” phase, with an EC_{50} value very similar to that of an HS-isoform $(\alpha 4)_2(\beta 2)_3$ -nAChR concatemeric construct (HSP; as shown in Fig. 5 and summarized in Table 1). This very closely resembles the 16% HS-like activity previously reported for LS $\alpha 4\beta 2$ -nAChR (expressed using biased ratios of un-linked $\alpha 4$ and $\beta 2$ subunits (Harpsoe et al., 2011)). The LS-phase function of the LSP construct had a $\log EC_{50}$ value of -4.39 ± 0.05 (or 41 μM). This was also very similar to the EC_{50} value (83 μM) recorded in the same study (Harpsoe et al., 2011), further confirming the suitability of the LSP construct as a model of LS $\alpha 4\beta 2$ -nAChR function. As hypothesized, the HS-like proportion of function was

significantly increased by mutations at the LSP $\alpha 4(+)/(-)\alpha 4$ subunit interface. This effect is shown in Fig. 5 (solid symbols), and summarized in Table 1. In addition, a subset of the mutated LSP mutants had significantly altered LS-phase EC_{50} values compared to the w.t. construct. Both constructs mutated in Loop C showed a significant drop in agonist potency (see Table 1). Surprisingly, ACh LS-phase potency was significantly higher at the Loop B Y184A mutant compared to the unmodified LSP construct (Table 1), which may indicate that structure / function relationships at the $\alpha 4(+)/(-)\alpha 4$ site are not completely conserved compared to those reported at $\alpha 4(+)/(-)\beta 2$ agonist binding sites. Overall, these findings support the concept that conserved residues at the LSP $\alpha 4(+)/(-)\alpha 4$ subunit interface are critical for LS-phase function under acute stimulation conditions.

Pretreatment with Saz-A eliminates the HS-phase of ACh-induced LSP function, and changes EC_{50} values of LS-phase responses:

Next, the same family of LSP constructs was pretreated with Saz-A (3.16 nM) for 5 min, before collection of ACh concentration-response curves. The most dramatic effect of pretreatment was to reduce the HS-phase responses of all LSP-variants to an undetectable level (Fig. 5, open symbols). This indicates that long-term agonist occupation of the conventional $\alpha 4(+)/(-)\beta 2$ agonist binding sites is sufficient to inactivate the HS-like phase of LSP function (which is therefore presumably mediated by the two $\alpha 4(+)/(-)\beta 2$ sites). By extension, it might be expected that the equivalent sites in an HSP construct would be similarly affected by long-term Saz-A incubation. Because of this, any residual ACh-induced function would have to be produced via a minority of HSP nAChR with unoccupied $\alpha 4(+)/(-)\beta 2$ sites. This should result in a smaller HSP response with no change in EC_{50} value (equivalent to the action of a non-competitive antagonist). As shown in Fig. 6, and Table 1, this is exactly what was observed.

Significantly, Saz-A occupation of the two LSP $\alpha 4(+)/(-)\beta 2$ agonist binding sites does change the EC_{50} of LS-phase responses (Fig. 6, Table 1). Thus, it seems that long-term

occupation of the two $\alpha 4(+)/(-)\beta 2$ sites permits subsequent receptor activation through binding to the additional $\alpha 4(+)/(-)\alpha 4$ site found only in LS $\alpha 4\beta 2$ -nAChR, but that this is accompanied by lowering of LS-phase agonist potency. Notably, the Saz-A-induced increase in the wild-type LS-phase ACh EC_{50} value as determined in these oocyte-electrophysiology experiments was very similar (approximately $\frac{1}{2}$ log unit) to that previously seen in the $^{86}Rb^+$ experiments. As shown in Table 1, lower LS-phase agonist potency following Saz-A pretreatment is consistently observed across all of the $\alpha 4(+)/(-)\alpha 4$ site mutants produced for this study. However, the magnitude of the Saz-A-induced loss of LS-phase ACh potency varies between the mutants (i.e. a significant Treatment x Mutation interaction was observed: see legend to Table 1).

A possible alternative explanation for the lower LS-phase ACh potency in the presence of Saz-A could be that Saz-A interacts with low affinity with the $\alpha 4(+)/(-)\alpha 4$ site, acting as a weak competitive antagonist. This was tested for by measuring the LS-phase ACh EC_{50} value following 5 min preincubation with a range of Saz-A concentrations. No systematic change in post-Saz-A LS-phase ACh EC_{50} value was observed, ruling out this possibility (at Saz-A concentrations of 1 nM 3.16 nM, 10 nM, and 31.6 nM, ACh $\log EC_{50}$ values were -4.13 ± 0.14 , -3.98 ± 0.04 , -4.02 ± 0.06 , and -4.00 ± 0.05 , respectively; Illustrated in Fig 7A). Another significant observation is that, for Saz-A concentrations ≥ 3.16 nM, the efficacy of LSP $\alpha 4\beta 2$ -nAChR LS-phase responses to ACh shows no consistent change (at Saz-A concentrations of 3.16 nM, 10 nM, and 31.6 nM, maximum ACh-induced responses were 23.1 ± 1.7 %, 14.3 ± 0.7 %, and 18.2 ± 2.0 % of the pre-Saz-A control, respectively). This plateau represents further evidence for a lack of Saz-A interaction at the $\alpha 4(+)/(-)\alpha 4$ site, even at the highest concentration tested (31.6 nM). In strong contrast, ACh-evoked responses at HSP $\alpha 4\beta 2$ -nAChR were greatly reduced following pre-exposure to 1 nM Saz-A, and were undetectable following pre-exposure to 31.6 nM Saz-A (Fig 7B).

Effects of $\alpha 4(+)/(-)\alpha 4$ site mutation on LSP HS-phase ACh EC_{50} values were also assessed (Table 1). Although HS-phase EC_{50} values were harder to measure precisely due to

the generally-smaller amounts of HS-phase function, a similar pattern emerged to that seen for the LS-phase: EC₅₀ values trend lower for Loop B mutants, and higher for Loop C mutants. However, a significant increase in HS-phase responses was only observed for the Y223A mutant (Table 1).

Effects of LSP $\alpha 4(+)/(-)\alpha 4$ subunit interface mutations on maximal ACh-induced function and surface expression:

Mutation of the LSP $\alpha 4(+)/(-)\alpha 4$ interface greatly affected the maximum amount of function (I_{\max}) that could be induced by ACh (Fig. 8A; note that the values shown in this panel are the sum of HS- and LS-phase function). Effects on I_{\max} could again be segregated according to which agonist-binding loop was mutated. Mutations in Loops A (Y126A) or C (Y223A, Y230A) reduced I_{\max} by > 90 % compared to the un-mutated LSP construct. In contrast, mutations in Loops B (W182A, Y184A) or D (W88A) reduced I_{\max} by no more than approximately half. For comparison, I_{\max} was also measured for oocytes expressing an HSP construct ($\beta 2-\alpha 4-\beta 2-\alpha 4-\beta 2$), and was observed to be significantly lower than that produced by the related, and non-mutated, LSP construct ($\beta 2-\alpha 4-\beta 2-\alpha 4-\alpha 4$). I_{\max} values for each construct are summarized in Table 2.

The observed changes in I_{\max} between LSP variants could be due to altered nAChR expression at the oocyte surface, altered amounts of function per unit of receptor, or a combination of both. Accordingly, we measured cell-surface nAChR expression using [¹²⁵I]mAb295 binding (Fig. 8B), for the same oocytes that were used in the I_{\max} determinations. Note that, as described in the Methods section, we compensated for the different $\beta 2$ subunit content of the HSP (3x $\beta 2$ subunits per receptor) vs. LSP constructs (2x $\beta 2$ subunits per receptor). Mutation-induced differences in nAChR protein expression on the cell surface (summarized in Table 2) are much less pronounced than are the accompanying changes in I_{\max} . In fact, although a trend can be observed towards lower surface expression by constructs harboring Loop A and C mutant subunits, one-way ANOVA showed no significant differences

compared to the unmodified LSP control (Table 2). Despite this apparent trend, when I_{\max} was normalized per unit of cell surface nAChR protein expression (Fig. 8C, Table 2), significant reductions in per-receptor I_{\max} were still noted for the LSP loop A and C mutants, compared to the unmodified LSP constructs. However, I_{\max} per receptor was not significantly changed by mutations in the B or D loops. These outcomes mirror closely the findings regarding I_{\max} only, demonstrating the dominant role of changes in “per receptor” function, as opposed to changes in surface expression, in mediating overall changes in I_{\max} .

By combining the normalized I_{\max} values with HS-fraction data from Table 1, it was possible to calculate the absolute amounts of HS-phase and LS-phase function per unit of cell-surface nAChR expression (Fig. 8C, black portions of the histogram show HS-phase function, white portions show LS-phase). Strikingly, two mutants produced increased HS-phase function (W88A in Loop D, W182A in loop B). For all other mutants, there was a trend towards reduced HS-phase function, although this did not quite reach significance (1-way ANOVA). Even more interestingly, I_{\max} / fmol surface-expressed receptor was indistinguishable between the HS-phase of the unmodified LSP construct and the HSP construct (which produces only HS-phase function).

Part of the I_{\max} response to acute ACh stimulation is mediated by HS-phase function, which is lost post-Saz-A treatment. Data from this study indicate that any agonist-induced LS-phase response of LSP nAChR is produced by an agonist interaction at the $\alpha 4/\alpha 4$ site. This is true whether the $\alpha 4/\beta 2$ sites are occupied long-term by a selective compounds such as Saz-A, or not (as in the case of a simple acute agonist challenge). Given this, it is arguably more legitimate to compare the magnitude of post-Saz-A responses to only the LS phase of the corresponding pre-Saz-A responses. For instance, 21 % of the pre-Saz-A LSP I_{\max} response shown in Fig. 4 is produced by HS-phase current. Thus LS-phase function represents only 79% of the LSP I_{\max} . When the maximum response is reduced following Saz-A pretreatment to 33% of the pre-Saz-A LSP I_{\max} control, given the elimination of the 21% contribution from the HS

phase, there is a 58% reduction in the LS phase of the response due to Saz-A pretreatment. Residual LS-only peak function thus corresponds to 42 % of the original LS-phase peak response. As shown in Fig. 9, the reduction in LS-phase function following Saz-A (3.16 nM) pretreatment is not significantly different across the set of LSP variants tested in this study (although several mutants appeared to show a trend towards a larger proportion of function retained).

DISCUSSION

The principal novel observation from this study is that pre-application of compounds that selectively interact with $\alpha 4(+)/\beta 2(-)$ agonist-binding sites preferentially diminishes HS- vs. LS-phase $\alpha 4\beta 2$ -nAChR function. Our results also show that the recently discovered $\alpha 4(+)/(-)\alpha 4$ subunit interface agonist binding site uniquely found in the LS isoform (Fig. 1) underlies this differential functional outcome. Since $\alpha 4\beta 2$ is the predominant neuronal nAChR subtype these discoveries are likely to have significant functional implications, and to provide important insights for drug discovery and development efforts.

The current findings concerning acute responses to A-85380 and Saz-A are consistent with previous reports. A-85380 agonist action at $\alpha 4\beta 2$ -nAChR has previously been shown to have a biphasic concentration-response relationship with > 100-fold higher potency at HS than LS $\alpha 4\beta 2$ -nAChR, and similar efficacy in both populations (Carbone et al., 2009; Marks et al., 1999). Similarly, our acute Saz-A stimulation data are consistent with prior observations that Saz-A is a full agonist at heterologously-expressed HS receptors and is poorly-efficacious at $\alpha 4\beta 2$ -nAChR (Kozikowski et al., 2009; Zwart et al., 2008). We demonstrate for the first time, using both loose-subunit and concatemeric approaches, that pretreatment with a low concentration of either A-85380 or Saz-A essentially abolishes HS-phase $\alpha 4\beta 2$ -nAChR responses to subsequent acute agonist applications. In contrast, the same pretreatment only induces a partial loss of subsequent LS-phase $\alpha 4\beta 2$ -nAChR agonist responses. This contrasts

with a previous study that indicated similar HS vs. LS desensitization potencies for a range of other nicotinic agonists (Marks et al., 2010). The different findings of the previous, and this present, study likely reflect the exceptional HS- vs. LS- $\alpha 4\beta 2$ -selectivity of A-85380 and Saz-A (presumably due to their strong preference for $\alpha 4(+)/(-)\beta 2$ over $\alpha 4(+)/(-)\alpha 4$ subunit agonist binding pockets).

Notably, function identified as LS-like in SH-EP1- $\alpha 4\beta 2$ cells was only reduced by 11 % following extended exposure to 3.16 nM Saz-A, while a greater effect was seen on LS-phase function of LSP nAChRs expressed in *Xenopus* oocytes. To some extent, this may reflect the uncertainty inherent in using least-squares curve fitting to separate HS from LS $\alpha 4\beta 2$ -nAChR function in the cell-line's mixed population. In addition it is important to note that $(\alpha 4)_3(\beta 2)_2$ -nAChR function contains an intrinsic component of HS-like activity. Because of this, the reported 67 % loss of LSP I_{\max} function measured in the oocyte experiments overestimates the effect of Saz-A pretreatment on the LS-only phase of function. Much of this difference is, however, likely due to the fact that peak inward current responses were measured in the oocyte electrophysiology experiments, whereas integrated function over five minutes was measured in the cell line $^{86}\text{Rb}^+$ experiments. Because of this, it seems likely that the two isoforms will be differentially affected by synaptically-released brief pulses of high concentration ACh (which will activate both isoforms) as opposed to by interaction with interstitial, volume transmitted ACh and / or exogenous nicotinic compounds. In the latter case, compounds will be present at much lower concentrations, and may also be present for significantly longer time scales than intra-synaptic ACh. Accordingly, the $^{86}\text{Rb}^+$ efflux measurements may be more applicable to the extrasynaptic context, in which cumulative function from longer-term stimulation may predominate over peak function. However, the central finding was that, in both the cell-line and oocyte experiments, across widely-different timescales, significantly more LS-phase vs. HS-phase $\alpha 4\beta 2$ -nAChR function was retained following exposure to the same concentration of Saz-A.

Our observations confirm the recent finding (Harpsoe et al., 2011) that approximately 20% of LS-isoform $\alpha 4\beta 2$ -nAChR function induced by ACh occurs in an HS-like phase. Whether HS $(\alpha 4)_2(\beta 2)_3$ vs. LS $(\alpha 4)_3(\beta 2)_2$ stoichiometry is enforced using either biased subunit expression ratios or linked-subunit approaches, HS functional expression is consistently lower than that of LS $\alpha 4\beta 2$ -nAChR (Carbone et al., 2009; Harpsøe et al., 2011; Mazzaferro et al., 2011; Nelson et al., 2003; Zhou et al., 2003; Zwart and Vijverberg, 1998). In this study we show, for the first time, that both isoforms express equally well at the cell surface. However, maximum function is approximately 5x greater on a “per receptor” basis for LS- vs. HS-isoform $\alpha 4\beta 2$ -nAChR (Fig. 8C). Interestingly, the HS:LS functional ratio is close to 1:1 across all mouse brain regions (Marks et al., 1999). This implies that the majority ($\approx 80\%$) of naturally-expressed $\alpha 4\beta 2$ -nAChR are of the $(\alpha 4)_2(\beta 2)_3$ stoichiometry, confirming earlier conclusions (Anand et al., 1991; Cooper et al., 1991). It is important to note that although HS:LS $\alpha 4\beta 2$ -nAChR functional ratios are similar across multiple brain regions, this does not necessarily mean that distributions of the isoforms are similar at the cellular or circuit level. In fact, observations of differing effects across multiple $\alpha 4\beta 2$ -nAChR-mediated behavioural measures for the LS isoform-selective positive allosteric modulator NS9283 (Timmermann et al., 2012) imply that this is not the case.

Intriguingly, the HS-phase response of LSP $\alpha 4\beta 2$ -nAChR is indistinguishable in magnitude from that of the total HSP response, on a per-receptor basis. This suggests that, for acute agonist stimulations, recruitment of the $\alpha 4(+)/(-)\alpha 4$ site at higher agonist concentrations acts to boost what would otherwise be similar function, mediated by the pair of $\alpha 4(+)/(-)\beta 2$ sites shared by both isoforms. Agonists binding at the $\alpha 4(+)/(-)\alpha 4$ site could, therefore, be considered to act similarly to positive allosteric modulators (PAMs). In fact Zn^{2+} has already been shown to be an allosteric activator of LS $\alpha 4\beta 2$ -nAChR by binding to different residues within the $\alpha 4(+)/(-)\alpha 4$ interface than those probed here (Moroni et al., 2008). Following long-term occupation of $\alpha 4(+)/(-)\beta 2$ sites by selective agonists such as A-85380 or Saz-A, it would seem likely that both

HS and LS $\alpha 4\beta 2$ -nAChR isoforms will become desensitized. The LS-phase responses evoked by subsequent agonist challenges at LS-isoform $\alpha 4\beta 2$ -nAChR would, in this understanding, be due to a reactivation of the desensitized LS-isoform nAChR through the previously-unbound $\alpha 4(+)/(-)\alpha 4$ site. In a further point of similarity, this could be considered to be analogous to the previously-reported activity of some PAMs at $\alpha 7$ nAChRs (Grønlien et al., 2007; Williams et al., 2011).

The presence of a third, functionally important, agonist site in a heteromeric nAChR is a relatively novel finding. However, this concept fits with findings regarding other members of the cysteine loop, ligand-gated ion channel (LGIC) superfamily. Of direct relevance, the $\alpha 1\beta$ -glycine receptor assembles with an $(\alpha 1)_3(\beta)_2$ subunit stoichiometry (Burzomato et al., 2003; Kuhse et al., 1993), and also seems to possess three functionally-relevant agonist binding sites (Burzomato et al., 2004). Further, two of these sites are likely located at earlier-identified $\alpha 1/\beta$ subunit interfaces, but the third site is likely located at the $\alpha 1/\alpha 1$ subunit interface, directly analogous to the nAChR $\alpha 4(+)/(-)\alpha 4$ subunit interface. Importantly, maximally-effective activation of homomeric $\alpha 7/5$ -HT3 chimeric receptors also requires activation of three agonist binding sites of the five available (Rayes et al., 2009). Additional, although less-directly-analogous, examples are provided by allosteric activators of LGICs. For GABA_A receptors, benzodiazepine allosteric actions are known to be mediated through drug interactions with a non-canonical α and γ subunit interface site (Sigel and Buhr, 1997). In addition, the partial agonist, morantel, potentiates acetylcholine-induced responses of $\alpha 3\beta 2$ -nAChR (Seo et al., 2009). The interpretation was that morantel interacts at non-canonical $\beta 2(+)/(-)\alpha 3$ interfaces, which would be analogous to nAChR $\beta 2(+)/(-)\alpha 4$ interfaces in the $\alpha 4\beta 2$ isoforms. Regardless of the fidelity with which functional and structural features of the recently-discovered $\alpha 4(+)/(-)\alpha 4$ -interface agonist binding site in LS $\alpha 4\beta 2$ -nAChR match those in other ligand-gated ion channels, the existence of additional functionally important subunit-interface binding sites

(outside of the set of long-recognized agonist binding pockets) seems to generalize across the LGIC superfamily.

Use of the LSP $\alpha 4\beta 2$ -nAChR construct enabled site-directed mutagenesis of critical residues only at the putative $\alpha 4(+)/(-)\alpha 4$ agonist binding pocket. This level of precision would not have been available if a non-linked subunit approach had been employed. The most notable and consistent effect of such mutations was to increase the ratio of HS- to LS-phase function compared to the unmodified LSP control (Fig. 5, Table 1). This observation is consistent with previous work (Mazzaferro et al., 2011), although that study failed to note the presence of an intrinsic HS-phase component within the wild-type $(\alpha 4)_3(\beta 2)_2$ response. Compared to the often-dramatic effects on LS-phase efficacy, mutation-induced changes in agonist LS-phase potency were relatively minor. This is also consistent with earlier work (Galzi et al., 1991) in which several equivalent residues were altered in $\alpha 7$ nAChR. Despite the fact that these mutations were introduced into five binding pockets (compared to only one here), most EC_{50} and IC_{50} shifts for competitive ligands were also quite limited (≈ 10 -fold or less). The surprising increase in LS-phase ACh potency for our Y184A mutant, however, suggests that there may be some fundamental structure/function differences between the recently-discovered $\alpha 4(+)/(-)\alpha 4$ site and previously-recognized agonist binding pockets. Such differences may prove useful for drug discovery/development work.

Our findings indicate a degree of functional interdependence between the pair of $\alpha 4(+)/(-)\beta 2$ sites and the $\alpha 4(+)/(-)\alpha 4$ site within each LS $\alpha 4\beta 2$ -nAChR. For example, the “per-receptor” amount of HS-phase function (presumably mediated by the $\alpha 4(+)/(-)\beta 2$ sites) can be decreased or even increased by individual mutations at the $\alpha 4(+)/(-)\alpha 4$ site. Conversely, persistent Saz-A occupation of the $\alpha 4(+)/(-)\beta 2$ sites reduces the efficacy and potency of LS $\alpha 4\beta 2$ -nAChR activation via the $\alpha 4(+)/(-)\alpha 4$ site. Determining the precise interplay between the three agonist sites within the LS isoform will likely require a great deal of further analysis, but should yield

fundamental insights into activation mechanisms for both nAChR and the wider LGIC superfamily.

The existence of HS and LS $\alpha 4\beta 2$ -nAChR isoforms has been known for over a decade. However, the relative distributions of HS and LS $\alpha 4\beta 2$ -nAChR isoforms within brain regions and across neuronal structures, and their physiological roles are not well understood. The results presented here illuminate receptor-level differences that underlie the differential pharmacology of the two $\alpha 4\beta 2$ -nAChR isoforms. They also illustrate that it is possible to selectively manipulate HS vs. LS $\alpha 4\beta 2$ -nAChR activity using pharmacological approaches. The unique, $\alpha 4(+)/(-)\alpha 4$ interface, ligand-binding site of LS $\alpha 4\beta 2$ -nAChR provides novel drug design opportunities. Examples could include competitive antagonists to selectively block LS $\alpha 4\beta 2$ -nAChR, agonists to selectively activate LS receptors, or compounds to “prime” LS receptors to effectively exhibit HS-like responses to endogenous acetylcholine. Such pharmacological tools could be used to uncover the physiological roles of HS vs. LS $\alpha 4\beta 2$ -nAChR. The compounds used in this study (A-85380 and Saz-A) may serve as useful lead molecules for the discovery of further HS vs. LS $\alpha 4\beta 2$ -nAChR selective compounds. As the predominant neuronal nAChR subtype, $\alpha 4\beta 2$ -nAChR are prominent targets for drug development and of existing smoking cessation therapies. Effects of existing compounds on HS and LS $\alpha 4\beta 2$ -nAChR isoforms often are not well characterized. However, the balance of activation/inactivation of HS- vs. LS-phase $\alpha 4\beta 2$ -nAChR function could be extremely important. Success in creation of superior aids to smoking cessation, and new nicotinic drugs for treatment of neurological or psychiatric disorders, involving $\alpha 4\beta 2$ -nAChR may depend on the selectivity of drug interactions with HS and LS $\alpha 4\beta 2$ isoforms.

ACKNOWLEDGEMENTS:

We thank Drs. F. Ivy Carroll (Research Triangle Institute, Research Triangle Park, NC) and Alan P. Kozikowski (University of Illinois, Chicago, IL) for gifts of compounds and Dr. Isabel

Bermudez (Oxford Brookes University, Oxford, UK) for providing the original HSP and LSP $\alpha 4\beta 2$ constructs that were modified for use in this study. We also thank Robert A. Ellingford (Placement Student, University of Bath, UK) and Dr. Andrew George (Research Assistant Professor, Barrow Neurological Institute, Phoenix, AZ) for excellent technical assistance.

AUTHORSHIP CONTRIBUTIONS:

Participated in research design: Lucero, Eaton, Stratton, Cooper, Chang, Lindstrom, Lukas, Whiteaker.

Conducted experiments: Lucero, Eaton, Stratton, Whiteaker.

Contributed new reagents or analytic tools: Lindstrom, Cooper

Performed data analysis: Lucero, Eaton, Stratton, Chang, Lukas, Whiteaker.

Wrote or contributed to the writing of the manuscript: Eaton, Lucero, Chang, Lukas, Lindstrom, Whiteaker.

REFERENCES

- Abreo MA, Lin N-H, Garvey DS, Gunn DE, Hettinger A-M, Wasicak JT, Pavlik PA, Martin YC, Donnelly-Roberts DL, Anderson DJ, Sullivan JP, Williams M, Arneric SP and Holladay MW (1996) Novel 3-Pyridyl Ethers with Subnanomolar Affinity for Central Neuronal Nicotinic Acetylcholine Receptors. *Journal of medicinal chemistry* **39**(4):817-825.
- Anand R, Conroy WG, Schoepfer R, Whiting P and Lindstrom J (1991) Neuronal nicotinic acetylcholine-receptors expressed in *Xenopus* oocytes have a pentameric quaternary structure *Journal of Biological Chemistry* **266**(17):11192-11198.
- Brejč K, van Dijk WJ, Smit AB and Sixma TK (2002) The 2.7 angstrom structure of AChBP, homologue of the ligand-binding domain of the nicotinic acetylcholine receptor, in *Ion Channels: from Atomic Resolution Physiology to Functional Genomics* pp 22-32.
- Burzomato V, Beato M, Groot-Kormelink PJ, Colquhoun D and Sivilotti LG (2004) Single-channel behavior of heteromeric alpha 1 beta glycine receptors: An attempt to detect a conformational change before the channel opens. *Journal of Neuroscience* **24**(48):10924-10940.
- Burzomato V, Groot-Kormelink PJ, Sivilotti LG and Beato M (2003) Stoichiometry of recombinant heteromeric glycine receptors revealed by a pore-lining region point mutation. *Recept Channels* **9**(6):353-361.
- Carbone AL, Moroni M, Groot-Kormelink PJ and Bermudez I (2009) Pentameric concatenated (alpha 4)(2)(beta 2)(3) and (alpha 4)(3)(beta 2)(2) nicotinic acetylcholine receptors: subunit arrangement determines functional expression. *British Journal of Pharmacology* **156**(6):970-981.
- Celie PHN, van Rossum-Fikkert SE, van Dijk WJ, Brejč K, Smit AB and Sixma TK (2004) Nicotine and carbamylcholine binding to nicotinic acetylcholine receptors as studied in AChBP crystal structures. *Neuron* **41**(6):907-914.
- Chang Y, Ghansah E, Chen Y, Ye J and Weiss DS (2002) Desensitization Mechanism of GABA Receptors Revealed by Single Oocyte Binding and Receptor Function. *The Journal of Neuroscience* **22**(18):7982-7990.
- Cooper E, Couturier S and Ballivet M (1991) Pentameric structure and subunit stoichiometry of a neuronal nicotinic acetylcholine-receptor *Nature* **350**(6315):235-238.
- Cordero-Erausquin M, Marubio LM, Klink R and Changeux JP (2000) Nicotinic receptor function: new perspectives from knockout mice. *Trends Pharmacol Sci* **21**(6):211-217.
- Corringer PJ, Le Novère N and Changeux JP (2000) Nicotinic receptors at the amino acid level. *Annual review of pharmacology and toxicology* **40**:431-458.
- Eaton JB, Peng JH, Schroeder KM, George AA, Fryer JD, Krishnan C, Buhlman L, Kuo YP, Steinlein O and Lukas RJ (2003) Characterization of human alpha 4 beta 2-nicotinic acetylcholine receptors stably and heterologously expressed in native nicotinic receptor-null SH-EP1 human epithelial cells. *Molecular pharmacology* **64**(6):1283-1294.
- Flores CM, Rogers SW, Pabreza LA, Wolfe BB and Kellar KJ (1992) A Subtype of Nicotinic Cholinergic Receptor in Rat-Brain Is Composed of Alpha-4-Subunit and Beta-2-Subunit and Is up-Regulated by Chronic Nicotine Treatment. *Molecular pharmacology* **41**(1):31-37.
- Galzi J-L, Bertrand D, Devillers-Thiéry A, Revah F, Bertrand S and Changeux J-P (1991) Functional significance of aromatic amino acids from three peptide loops of the $\alpha 7$ neuronal nicotinic receptor site investigated by site-directed mutagenesis. *Febs Letters* **294**(3):198-202.
- Gentry CL, Wilkins LH and Lukas RJ (2003) Effects of prolonged nicotinic ligand exposure on function of heterologously expressed, human alpha 4 beta 2-and alpha 4 beta 4-nicotinic acetylcholine receptors. *Journal of Pharmacology and Experimental Therapeutics* **304**(1):206-216.

- Gotti C, Clementi F, Fornari A, Gaimarri A, Guiducci S, Manfredi I, Moretti M, Pedrazzi P, Pucci L and Zoli M (2009) Structural and functional diversity of native brain neuronal nicotinic receptors. *Biochem Pharmacol* **78**(7):703-711.
- Gotti C, Moretti M, Meinerz NM, Clementi F, Gaimarri A, Collins AC and Marks MJ (2008) Partial deletion of the nicotinic cholinergic receptor alpha 4 or beta 2 subunit genes changes the acetylcholine sensitivity of receptor-mediated Rb-86(+) efflux in cortex and thalamus and alters relative expression of alpha 4 and beta 2 subunits. *Molecular pharmacology* **73**(6):1796-1807.
- Grønlien JH, Håkerud M, Ween H, Thorin-Hagene K, Briggs CA, Gopalakrishnan M and Malysz J (2007) Distinct Profiles of $\alpha 7$ nAChR Positive Allosteric Modulation Revealed by Structurally Diverse Chemotypes. *Molecular pharmacology* **72**(3):715-724.
- Harpsøe K, Ahring PK, Christensen JK, Jensen ML, Peters D and Balle T (2011) Unraveling the High- and Low-Sensitivity Agonist Responses of Nicotinic Acetylcholine Receptors. *The Journal of Neuroscience* **31**(30):10759-10766.
- Kozikowski AP, Eaton JB, Bajjuri KM, Chellappan SK, Chen Y, Karadi S, He R, Caldarone B, Manzano M, Yuen P and Lukas RJ (2009) Chemistry and pharmacology of new nicotinic ligands based on 6-[5-(azetidin-2-ylmethoxy)pyridin-3-yl]hex-5-yn-1-ol (AMOP-H-OH, aka sazetidine-A) for possible use in depression. *Chem Med Chem* **4**:1279-1291.
- Kuhse J, Laube B, Magalei D and Betz H (1993) Assembly of the inhibitory glycine receptor - identification of amino-acid-sequence motifs governing subunit stoichiometry *Neuron* **11**(6):1049-1056.
- Kuryatov A and Lindstrom J (2011) Expression of Functional Human alpha6beta2beta3* Acetylcholine Receptors in *Xenopus laevis* Oocytes Achieved through Subunit Chimeras and Concatamers. *Molecular pharmacology* **79**(1):126-140.
- Lai A, Parameswaran N, Khwaja M, Whiteaker P, Lindstrom JM, Fan H, McIntosh JM, Grady SR and Quik M (2005) Long-term nicotine treatment decreases striatal alpha 6 nicotinic acetylcholine receptor sites and function in mice. *Molecular pharmacology* **67**(5):1639-1647.
- Lindstrom JM (2003) Nicotinic acetylcholine receptors of muscles and nerves - Comparison of their structures, functional roles, and vulnerability to pathology, in *Myasthenia Gravis and Related Disorders* pp 41-52.
- Lukas RJ and Cullen MJ (1988) An isotopic rubidium ion efflux assay for the functional characterization of nicotinic acetylcholine receptors on clonal cell lines. *Analytical Biochemistry* **175**(1):212-218.
- Marks MJ, Meinerz NM, Brown RWB and Collins AC (2010) 86Rb+ efflux mediated by [alpha]4[beta]2*-nicotinic acetylcholine receptors with high and low-sensitivity to stimulation by acetylcholine display similar agonist-induced desensitization. *Biochemical pharmacology* **80**(8):1238-1251.
- Marks MJ, Whiteaker P, Calcaterra J, Stitzel JA, Bullock AE, Grady SR, Picciotto MR, Changeux JP and Collins AC (1999) Two pharmacologically distinct components of nicotinic receptor-mediated rubidium efflux in mouse brain require the beta 2 subunit. *Journal of Pharmacology and Experimental Therapeutics* **289**(2):1090-1103.
- Mazzaferro S, Benallegue N, Carbone A, Gasparri F, Vijayan R, Biggin PC, Moroni M and Bermudez I (2011) Additional Acetylcholine (ACh) Binding Site at $\alpha 4/\alpha 4$ Interface of ($\alpha 3\beta 2$) $2\alpha 4$ Nicotinic Receptor Influences Agonist Sensitivity. *Journal of Biological Chemistry* **286**(35):31043-31054.
- Moroni M, Vijayan R, Carbone A, Zwart R, Biggin PC and Bermudez I (2008) Non-agonist-binding subunit interfaces confer distinct functional signatures to the alternate stoichiometries of the alpha 4 beta 2 nicotinic receptor: An alpha 4-alpha 4 interface is required for Zn2+ potentiation. *Journal of Neuroscience* **28**(27):6884-6894.

- Nelson ME, Kuryatov A, Choi CH, Zhou Y and Lindstrom J (2003) Alternate stoichiometries of alpha 4 beta 2 nicotinic acetylcholine receptors. *Molecular pharmacology* **63**(2):332-341.
- Picciotto MR, Zoll M, Lena C, Bessis A, Lallemant Y, Lenovere N, Vincent P, Pich EM, Brulet P and Changeux JP (1995) Abnormal Avoidance-Learning in Mice Lacking Functional High-Affinity Nicotine Receptor in the Brain. *Nature* **374**(6517):65-67.
- Rayes D, De Rosa MJ, Sine SM and Bouzat C (2009) Number and Locations of Agonist Binding Sites Required to Activate Homomeric Cys-Loop Receptors. *Journal of Neuroscience* **29**(18):6022-6032.
- Seo S, Henry JT, Lewis AH, Wang N and Levandoski MM (2009) The Positive Allosteric Modulator Morantel Binds at Noncanonical Subunit Interfaces of Neuronal Nicotinic Acetylcholine Receptors. *Journal of Neuroscience* **29**(27):8734-8742.
- Sigel E and Buhr A (1997) The benzodiazepine binding site of GABA(A) receptors. *Trends Pharmacol Sci* **18**(11):425-429.
- Steinlein OK (2001) Genes and mutations in idiopathic epilepsy. *American Journal of Medical Genetics* **106**(2):139-145.
- Timmermann DB, Sandager-Nielsen K, Dyhring T, Smith M, Jacobsen AM, Nielsen E, Grunnet M, Christensen JK, Peters D, Kohlhaas K, Olsen GM and Ahring PK (2012) Augmentation of cognitive function by NS9283, a stoichiometry-dependent positive allosteric modulator of $\alpha 2$ - and $\alpha 4$ -containing nicotinic acetylcholine receptors. *British Journal of Pharmacology* **167**(1):164-182.
- Whiteaker P, Cooper JF, Salminen O, Marks MJ, McClure-Begley TD, Brown RWB, Collins AC and Lindstrom JM (2006) Immunolabeling demonstrates the interdependence of mouse brain $\alpha 4$ and $\beta 2$ nicotinic acetylcholine receptor subunit expression. *The Journal of comparative neurology* **499**(6):1016-1038.
- Whiteaker P, Wilking JA, Brown RWB, Brennan RJ, Collins AC, Lindstrom JM and Boulter J (2009) Pharmacological and immunochemical characterization of $\alpha 2^*$ nicotinic acetylcholine receptors (nAChRs) in mouse brain. *Acta Pharmacol Sin* **30**(6):795-804.
- Whiting P and Lindstrom J (1987) Purification and Characterization of a Nicotinic Acetylcholine-Receptor from Rat-Brain. *Proceedings of the National Academy of Sciences of the United States of America* **84**(2):595-599.
- Whiting P and Lindstrom J (1988) Characterization of bovine and human neuronal nicotinic acetylcholine receptors using monoclonal antibodies. *The Journal of Neuroscience* **8**(9):3395-3404.
- Williams DK, Wang J and Papke RL (2011) Investigation of the Molecular Mechanism of the $\alpha 7$ Nicotinic Acetylcholine Receptor Positive Allosteric Modulator PNU-120596 Provides Evidence for Two Distinct Desensitized States. *Molecular pharmacology* **80**(6):1013-1032.
- Xiao YX, Fan H, Musachio JL, Wei ZL, Chellappan SK, Kozikowski AP and Kellar KJ (2006) Sazetidine-a, a novel ligand that desensitizes alpha 4 beta 2 nicotinic acetylcholine receptors without activating them. *Molecular pharmacology* **70**(4):1454-1460.
- Xiu X, Puskar NL, Shanata JAP, Lester HA and Dougherty DA (2009) Nicotine binding to brain receptors requires a strong cation-pi interaction. *Nature* **458**(7237):534-537.
- Zhou Y, Nelson ME, Kuryatov A, Choi C, Cooper J and Lindstrom J (2003) Human alpha 4 beta 2 acetylcholine receptors formed from linked Subunits. *Journal of Neuroscience* **23**(27):9004-9015.
- Zwart R, Carbone AL, Moroni M, Bermudez I, Mogg AJ, Folly EA, Broad LM, Williams AC, Zhang D, Ding C, Heinz BA and Sher E (2008) Sazetidine-A is a potent and selective agonist at native and recombinant alpha 4 beta 2 nicotinic acetylcholine receptors. *Molecular pharmacology* **73**(6):1838-1843.

Zwart R and Vijverberg HPM (1998) Four pharmacologically distinct subtypes of alpha 4 beta 2 nicotinic acetylcholine receptor expressed in *Xenopus laevis* oocytes. *Molecular pharmacology* **54**(6):1124-1131.

FOOTNOTES

This work was primarily supported by National Institutes of Health grant [DA026627] to P.W., with additional funding from National Institutes of Health awards [DA012242] (to P.W.), [MH085193], [DA015389], [DA017980], [DA019375], [DA019377], (to R.J.L.), [NS011323] (to J.M.L.), and [GM085237] (to Y.C.). The contents of this article do not necessarily reflect the views of the aforementioned awarding agencies.

Please send reprint requests to Paul Whiteaker, Ph.D., Laboratory of Neurochemistry, Division of Neurobiology, Barrow Neurological Institute, 350 West Thomas Road, Phoenix, AZ 85013. Email: paul.whiteaker@dignityhealth.org

[†]J.B.E. and L.M.L. contributed equally to this work.

FIGURE LEGENDS

Figure 1. Schematic diagrams of concatenated HS and LS $\alpha 4\beta 2$ -nAChR isoform pentameric constructs (HSP and LSP, respectively). A: At the cDNA level, individual subunits are joined using linkers that encode AGS repeats. Each linker also contains a unique restriction site (noted at the base of panel A). These sites allow rapid removal and replacement of individual subunits by a simple restriction digestion and ligation approach (Carbone et al., 2009). For both HSP and LSP, long-recognized agonist binding pockets form at the interfaces between the principal (+) faces of $\alpha 4$ subunits in positions 2 and 4, and the complementary (-) faces of $\beta 2$ subunits in positions 1 and 3, respectively. The functional pharmacology implications of the further, LSP-unique, agonist binding pocket between the (+) face of $\alpha 4$ position 5 and the (-) face of $\alpha 4$ position 4 are explored in this study; site-directed mutant $\alpha 4$ subunits were substituted in positions 4 and 5 of the original LSP construct. B: Schematic of an assembled HSP $\alpha 4\beta 2$ -nAChR, showing the arrangement of the subunit + and – interfaces, the resulting pair of agonist binding pockets, and the linkers. C: Schematic of an assembled LSP $\alpha 4\beta 2$ -nAChR. Note that much of the structure is similar to the HSP isoform, but that an $\alpha 4$ subunit is substituted for the $\beta 2$ subunit in position 5. This gives rise to the additional agonist binding site shown between the 4th and 5th subunits of LSP $\alpha 4\beta 2$ -nAChR.

Figure 2. Ligand-specific activation or desensitization of $\alpha 4\beta 2$ -nAChR. SH-EP1-h $\alpha 4\beta 2$ cells stably expressing functional, human $\alpha 4\beta 2$ -nAChR from loose subunits were subjected to acute challenges for 5 min with the indicated drugs at the specified concentrations (abscissa; log M scale) for determination of specific $^{86}\text{Rb}^+$ efflux (defined in Methods; ordinate; % of control response to a full agonist, 1 mM carbamylcholine). A: Acute response to Saz-A (●). B: Acute response to A-85380 (●). C: Acute response to Saz-A after 10 min pretreatment with 3.16 nM Saz-A (◆) or A-85380 (◇). D: Acute response to A-85380 after 10 min pretreatment with 3.16 nM Saz-A (◆) or A-85380 (◇). Results were fit to unconstrained,

one- or two-site logistic equations. The derived $\log EC_{50}$ values, Hill coefficients, and fractional contributions of each site (in the case of two-site fits) are reported in the text.

Figure 3. Acute Saz-A and A-85380 stimulation of HSP vs. LSP $\alpha 4\beta 2$ -nAChR expressed in *Xenopus* oocytes. *Xenopus laevis* oocytes expressing human HSP and LSP $\alpha 4\beta 2$ -nAChR constructs were acutely stimulated with the indicated range of Saz-A (Panel A) or A-85380 (Panel B) concentrations. Values are mean \pm SEM, $n = 3$ individual determinations, and are reported as % of maximally-efficacious ACh control responses (experimental details in Methods). Results were fit to unconstrained one-site logistic equations. The derived agonist $\log EC_{50}$, Hill coefficient, and efficacy values are reported in the text.

Figure 4. Saz-A pretreatment effects on HSP vs. LSP $\alpha 4\beta 2$ -nAChR function. *Xenopus* oocytes injected with mRNA encoding either wild-type HSP $\alpha 4\beta 2$ -nAChR or wild-type LSP $\alpha 4\beta 2$ -nAChR were tested for the effects of Saz-A (5 min) pretreatment on subsequent, acute, agonist stimulation. Initial control stimulation was performed for 1 s, using a maximally-effective concentration of ACh (30 μ M for HSP, 1 mM for LSP). Oocytes were then exposed to Saz-A (3.16 nM) for 5 min, and the ACh challenge was repeated (1 s stimulation, co-applied with 3.16 nM Saz-A); typical traces are shown. Saz-A pretreatment greatly reduced HSP responses (peak response diminished to 17.6 ± 2.1 %; mean \pm s.e.m., $n = 4$). In contrast, Saz-A pretreatment diminished LSP peak responses to 33.3 ± 3.0 % (mean \pm s.e.m., $n = 4$). The difference in response to Saz-A pretreatment between HSP and LSP was significant (Student's unpaired two-tailed t-test; $t = 4.21$ with 6 degrees of freedom, $P < 0.01$).

Figure 5. ACh activation of wild-type vs. mutant LSP $\alpha 4\beta 2$ -nAChR. *Xenopus* oocytes injected with unmodified or mutant LSP mRNA were exposed to acute ACh challenges (1 s, concentrations specified on the X-axis; log M scale). Filled symbols show concentration response relationships determined for each LSP variant when exposed to acute ACh stimulation. Note that the proportion of HS-phase function is enhanced for every LSP mutant

compared to the unmodified LSP construct. Open symbols depict concentration response determinations for the same constructs, when exposed to a range of ACh concentrations following 5 min preincubation with Saz-A (3.16 nM, 5 min). Pretreatment with Saz-A reduced HS-phase function of all LSP variants to such an extent that it could no longer be fit as part of a two-site model, leaving only LS-phase function. Log EC₅₀ values for HS- and LS-phase responses, fractions of HS- vs. LS-phase function, and statistical analyses are reported in Table 1. Points are mean ± SEM, n = 6 – 12).

Figure 6. Pretreatment with Saz-A eliminates the HS-phase of ACh-induced LSP function, and changes the EC₅₀ of LS-phase responses. *Xenopus* oocytes injected with unmodified HSP (squares) and LSP (circles) mRNA were exposed to acute ACh challenges (1 s, concentrations specified on the X-axis; log M scale), before (filled symbols) and after (open symbols) pre-treatment with Saz-A (3.16 nM, 5 min). All concentration-response data are normalized to the maximum response measured for each concentration series, in each oocyte (mean ± SEM, n = 8-12). For HSP α4β2-nAChR, no change in ACh EC₅₀ value was seen following preincubation with Saz-A. For LSP α4β2-nAChR, the HS-phase of the CRC (below ≈10^{-5.5} M) was abolished by preincubation with Saz-A, while the potency of the LS-phase response was reduced. Log EC₅₀ values for HS- and LS-phase responses, fractions of HS- vs. LS-phase function, and statistical analyses are reported in Table 1.

Figure 7. Effects of changing Saz-A preincubation concentration on LSP and HSP ACh-induced responses. *Xenopus* oocytes injected with unmodified LSP (Panel A) and HSP (Panel B) mRNA were first exposed to a maximally-effective ACh control challenge, followed by pretreatment with Saz-A (5 min, concentrations indicated in legends). Concentration response data were then collected using a series of acute ACh challenges (1 s, concentrations specified on the X-axis; log M scale, see Methods for details). All concentration-response data were normalized to the initial control stimulation, in each oocyte

(mean \pm SEM, $n = 3$). For LSP $\alpha 4\beta 2$ -nAChR, Saz-A preincubation reduced (1 nM), then abolished (>3.16 nM) HS-phase responses. ACh EC_{50} values and magnitudes of LS-phase responses were unaffected by increasing Saz-A preincubation concentrations (3.16 – 31.6 nM; pharmacological parameters reported in the text). For HSP $\alpha 4\beta 2$ -nAChR, ACh responses were reduced by 1 nM Saz-A preincubation but, in contrast to LSP responses, no function remained following 31.6 nM Saz-A preincubation.

Figure 8. LSP $\alpha 4(+)/(-)\alpha 4$ interface mutation effects on maximum peak ACh-induced function (I_{max}) and nAChR cell-surface expression. *Xenopus* oocytes were injected with mRNAs encoding either unmodified or mutant LSP constructs (Loop A Y126A; Loop B W182A, Y184A; Loop C Y223A, Y230A; Loop D W88A), or an unmodified HSP construct (see Methods for details). Panel A: Maximum peak ACh-induced function (I_{max}) was determined for each construct. I_{max} is significantly reduced by several of the mutations compared to the unmodified LSP construct, and the HSP construct also has a significantly lower I_{max} value than that recorded for the wild-type LSP construct (* $p < 0.05$; *** $p < 0.001$). Panel B: nAChR protein expression at the surface of *Xenopus* oocytes was determined using an [125 I]mAb295 binding assay. Note, binding of two [125 I]mAb295 molecules per LSP construct and three per HSP construct (reflecting the different $\beta 2$ subunit numbers in each nAChR isoform; see Methods) was assumed. Although some apparent variation in nAChR cell-surface expression was observed across the tested constructs, this did not reach the level of statistical significance. Panel C: I_{max} values were normalized to the amounts of nAChR cell-surface expression for each construct. By applying the HS-phase function fractions calculated for each construct (Table 1), it was possible to determine the absolute amount of HS- and LS-phase function for each construct. Significant changes are noted for HS-phase function by ** ($p < 0.01$) or *** ($p < 0.001$), and for overall function (I_{max}) by + ($p < 0.05$) or ++ ($p < 0.01$). Note, the HSP result was not included in the overall function comparison for Panel C, since this

construct produces only HS-phase function. Details of the analysis applied, and parameter values determined, are supplied in Table 2.

Figure 9. Comparison of Saz-A pretreatment effects on LS-phase function across LSP variants.

Xenopus oocytes were injected with unmodified and mutant LSP mRNAs. ACh concentration-response experiments were performed to determine maximal LS-phase function before and after pre-treatment with Saz-A (3.16 nM, 5 min). The percentage of post- vs. pre-treatment LS-phase function is displayed for each LSP variant construct used in this study. Values shown are the mean \pm SEM of 6-8 individual determinations collected from three separate experiments. One-way ANOVA showed no significant differences across the LSP variants ($F[6,14] = 1.85$, $p = 0.16$).

Table 1. Agonist stimulation parameters: ACh activation of unmodified vs. mutant LSP $\alpha 4\beta 2$ -nAChR.

Concatemer	Mutation site	ACh only		ACh Post-Saz-A		n	n
		Log (M) EC ₅₀ (HS)	HS Fraction	Log (M) EC ₅₀ (LS)	Log (M) EC ₅₀ (LS)		
$\beta 2$ - $\alpha 4$ - $\beta 2$ - $\alpha 4$ - $\alpha 4$ (LSP)	--	-6.44 \pm 0.26	0.21 \pm 0.03	-4.39 \pm 0.05	-3.94 \pm 0.03	12	8
$\beta 2$ - $\alpha 4$ - $\beta 2$ - $\alpha 4$ ^{W88A} - $\alpha 4$	Loop D	-6.39 \pm 0.08	0.51 \pm 0.02***	-4.13 \pm 0.06	-3.77 \pm 0.05	9	6
$\beta 2$ - $\alpha 4$ - $\beta 2$ - $\alpha 4$ ^{Y126A} - $\alpha 4$	Loop A	-5.87 \pm 0.09	0.40 \pm 0.03**	-4.21 \pm 0.05	-3.83 \pm 0.04	9	6
$\beta 2$ - $\alpha 4$ - $\beta 2$ - $\alpha 4$ ^{W182A} - $\alpha 4$	Loop B	-6.75 \pm 0.08	0.65 \pm 0.02***	-4.44 \pm 0.08	-3.76 \pm 0.05*	9	6
$\beta 2$ - $\alpha 4$ - $\beta 2$ - $\alpha 4$ ^{Y184A} - $\alpha 4$	Loop B	-6.68 \pm 0.18	0.29 \pm 0.03	-4.92 \pm 0.05***	-4.05 \pm 0.04	9	6
$\beta 2$ - $\alpha 4$ - $\beta 2$ - $\alpha 4$ ^{Y223A} - $\alpha 4$	Loop C	-5.62 \pm 0.14*	0.42 \pm 0.04***	-3.74 \pm 0.08***	-3.42 \pm 0.05***	9	6
$\beta 2$ - $\alpha 4$ - $\beta 2$ - $\alpha 4$ ^{Y230A} - $\alpha 4$	Loop C	-5.77 \pm 0.21	0.29 \pm 0.05	-4.06 \pm 0.07*	-3.56 \pm 0.05***	9	6
$\beta 2$ - $\alpha 4$ - $\beta 2$ - $\alpha 4$ - $\beta 2$ (HSP)	--	-5.56 \pm 0.04	1	--	-5.36 \pm 0.05	5	8

Unmodified and mutant LSP construct mRNAs were expressed in *Xenopus* oocytes. ACh CRCs were performed either in the absence or presence of Saz-A preincubation (3.16 nM, 5 min). Oocytes were also injected with HSP mRNA for comparison to the LSP variants. Details are provided in the legend of Figure 5, and in the Methods section. HS- and LS-phase $\log_{10}(\text{EC}_{50} / \text{M})$, and fraction of HS-phase function were determined by least-squares curve fitting where possible (Saz-A preincubation rendered HS-phase function unmeasurable for all constructs). Numbers of individual oocytes tested are shown in the table (n= 6-12; derived from three separate experiments). All values are given as mean \pm S.E.M. Initially, two-way ANOVA was performed to determine the effect of Mutation and Treatment on the LS-phase EC₅₀ values of the LSP construct ACh concentration response curves. Both factors significantly affected the observed EC₅₀ values ($F[6,28] = 53.8$, $p < 0.001$, and ($F[1,28] = 300$, $p < 0.001$), respectively, and a significant Mutation x Treatment interaction was also seen ($F[6,28] = 6.54$, $p < 0.001$).

For LS-phase EC₅₀ values determined only with acute ACh exposure, ACh potency at the Loop B Y184A mutant was significantly increased, while potency at the two C-loop mutants (Y223A, Y230A) was significantly reduced compared to the unmodified LSP control (One-way ANOVA with Dunnett's post hoc test ($F[6,20] = 33.1$, $p < 0.001$); individual mutant differences from control are denoted as * $p < 0.05$, *** $p < 0.001$).

For residual LS-like responses measured following Saz-A preincubation, statistically significant decreases in ACh potency compared to the unmodified LSP control construct were observed for three mutants (One-way ANOVA with Dunnett's post hoc test ($F[6,20] = 24.0$, $p < 0.001$; individual mutant differences from control are denoted as * $p < 0.05$, *** $p < 0.001$).

The fraction of HS-phase function, and ACh EC_{50} values for this function were determined before pre-treatment with Saz-A (HS-phase responses were undetectable following pre-treatment). A highly-significant overall increase in the HS fraction was seen across the set of mutations (One-way ANOVA, $F[6,20] = 22.8$, $p < 0.001$; individual mutant differences from control were determined using Dunnett's post-hoc testing and are denoted as ** $p < 0.01$, *** $p < 0.001$). Again, ACh potency was reduced compared to the unmodified LSP control construct by one of the C-loop mutants (Y223A; One-way ANOVA $F[6,20] = 7.83$, with Dunnett's post hoc test showing * $p < 0.05$).

Table 2. Effects of $\alpha 4(-)/(+)\alpha 4$ agonist binding site mutations on LSP construct function and cell-surface expression.

Concatemer	Mutation site	ACh I_{\max} (nA)	Specific [125 I]mAb 295 binding (fmol/oocyte)	N	HS-phase (μ A/fmol)	LS-phase (μ A/fmol)
$\beta 2-\alpha 4-\beta 2-\alpha 4$ (LSP)	--	3100 ± 530	0.036 ± 0.005	5	19.9 ± 5.8	75.7 ± 19.8
$\beta 2-\alpha 4-\beta 2-\alpha 4^{W88A}$	Loop D	2700 ± 920	0.030 ± 0.003	3	$50.2 \pm 12.1^{**}$	48.1 ± 11.4
$\beta 2-\alpha 4-\beta 2-\alpha 4^{Y126A}$	Loop A	$300 \pm 50^{**}$	0.017 ± 0.001	3	7.2 ± 1.6	$10.9 \pm 2.3^*$
$\beta 2-\alpha 4-\beta 2-\alpha 4^{W182A}$	Loop B	3700 ± 670	0.053 ± 0.018	3	$65.8 \pm 9.0^{***}$	36.2 ± 4.8
$\beta 2-\alpha 4-\beta 2-\alpha 4^{Y184A}$	Loop B	1900 ± 170	0.032 ± 0.005	3	19.7 ± 4.5	49.1 ± 10.2
$\beta 2-\alpha 4-\beta 2-\alpha 4^{Y223A}$	Loop C	$220 \pm 30^{**}$	0.021 ± 0.003	3	4.6 ± 0.9	$6.4 \pm 1.1^*$
$\beta 2-\alpha 4-\beta 2-\alpha 4^{Y230A}$	Loop C	$120 \pm 30^{**}$	0.016 ± 0.001	3	2.3 ± 0.8	$5.5 \pm 1.7^{**}$
$\beta 2-\alpha 4-\beta 2-\alpha 4-\beta 2$ (HSP)	--	$710 \pm 60^*$	0.039 ± 0.003	3	18.4 ± 2.8	Not applicable

Un-modified and mutant LSP, and HSP, nAChR construct mRNAs were expressed in *Xenopus* oocytes. ACh CRCs were performed in the absence of Saz-A preincubation. Maximum function (I_{\max}), and the fraction of HS-phase function, were determined by least-squares curve fitting. Surface expression of nAChR was then determined for the same oocytes using [125 I]mAb295 binding (see Methods section). Data were collected from N = 3-5 individual experiments, with six oocytes tested per condition in each experiment. All values are given as mean \pm S.E.M. One-way ANOVA was used to test within each measure for differences from control (un-modified LSP) parameters, with Dunnett's post-hoc test used to identify individual constructs that differed from control (* $p < 0.05$, ** $p < 0.01$, *** $p < 0.001$). Overall ANOVA results showed significant differences in overall I_{\max} (sum of HS- and LS-phase function; $F[7,17] = 8.43$, $p = 0.0002$), and also in surface expression levels ($F[7,17] = 3.101$, $p = 0.025$ although post-hoc testing failed to identify differences vs. the unmodified LSP control for the HSP or for any of the mutant LSP constructs). Overall (I_{\max}) function was subdivided into HS- and LS-phase responses for each construct where possible (no LS-phase function was produced by HSP nAChR), and normalized to nAChR surface expression levels. Significant differences were seen in both normalized HS-phase function ($F[7,17] = 12.6$, $p < 0.0001$; two constructs showed increased HS-phase function), and in normalized LS-phase function ($F[6,16] = 4.57$, $p = 0.0069$,

all constructs showed a trend to decreased LS-phase function, with three reaching statistical significance).

Figure 1

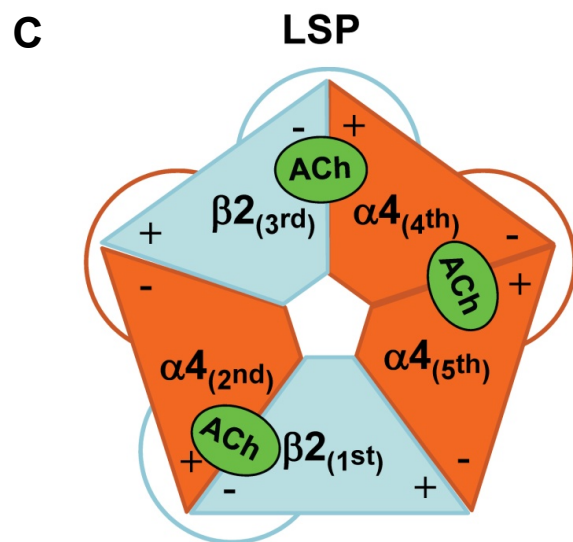
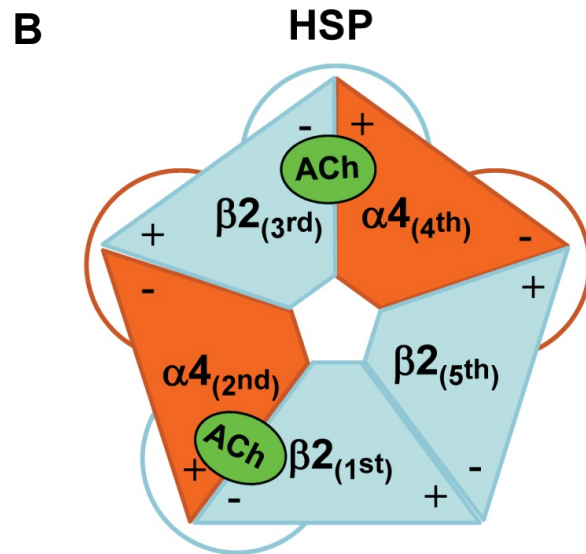
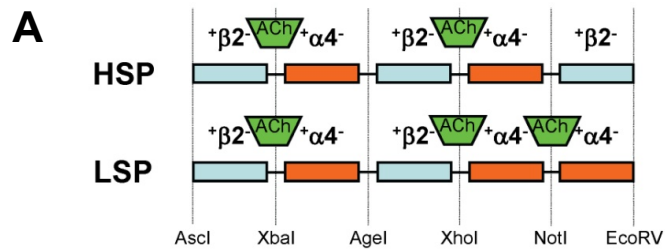


Figure 2

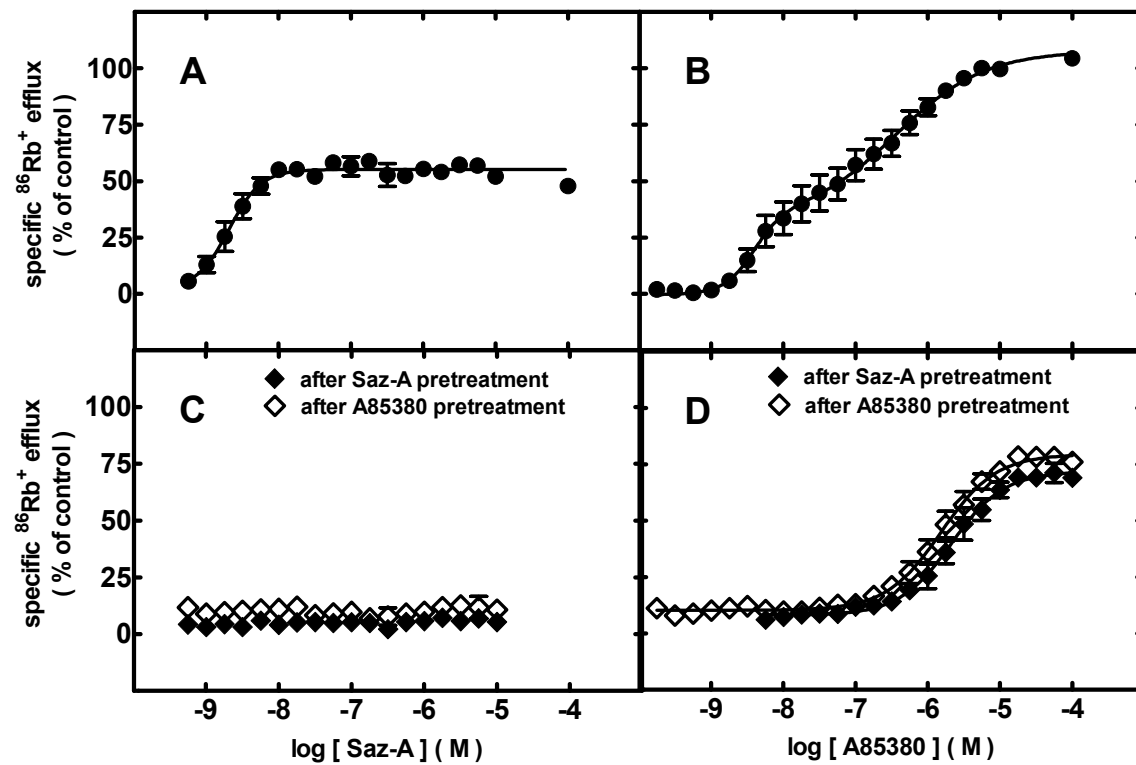


Figure 3

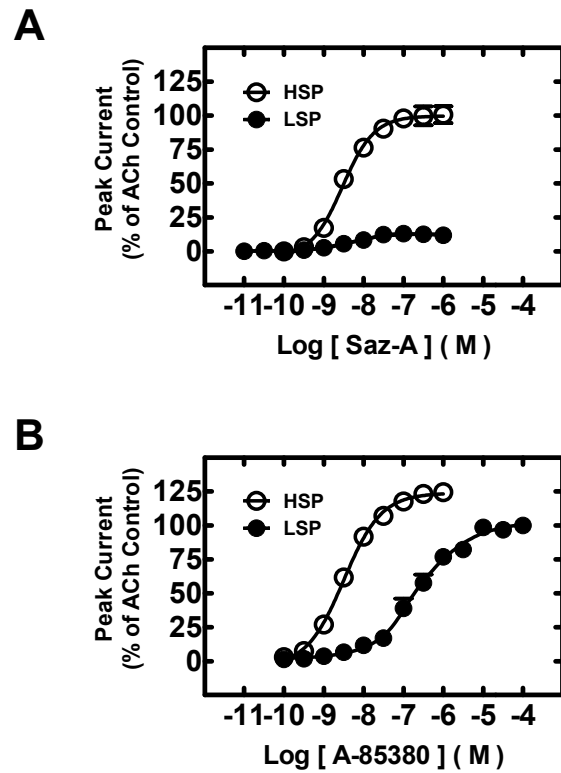


Figure 4

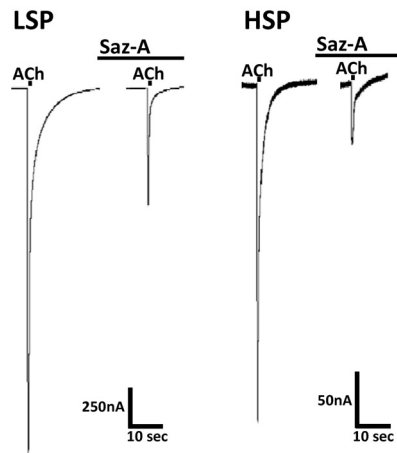


Figure 5

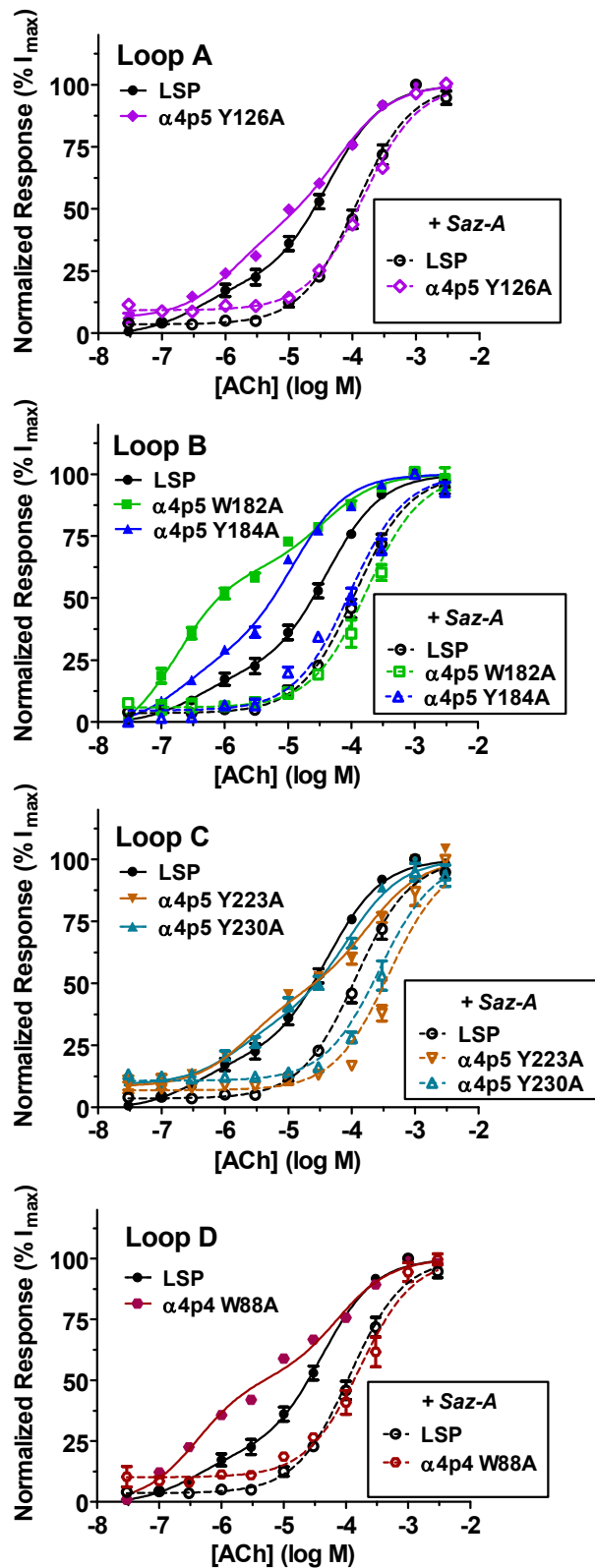


Figure 6

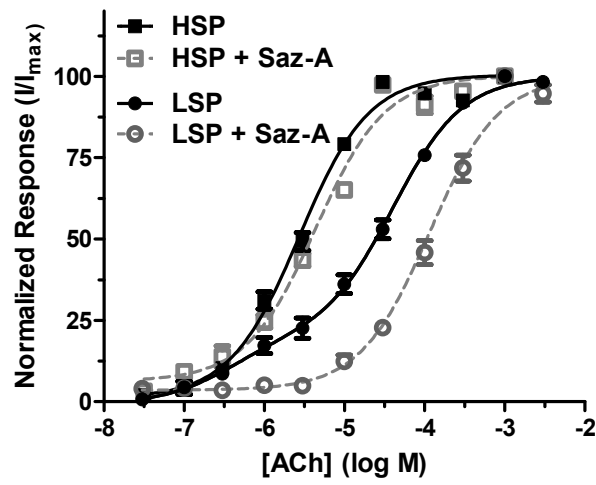


Figure 7

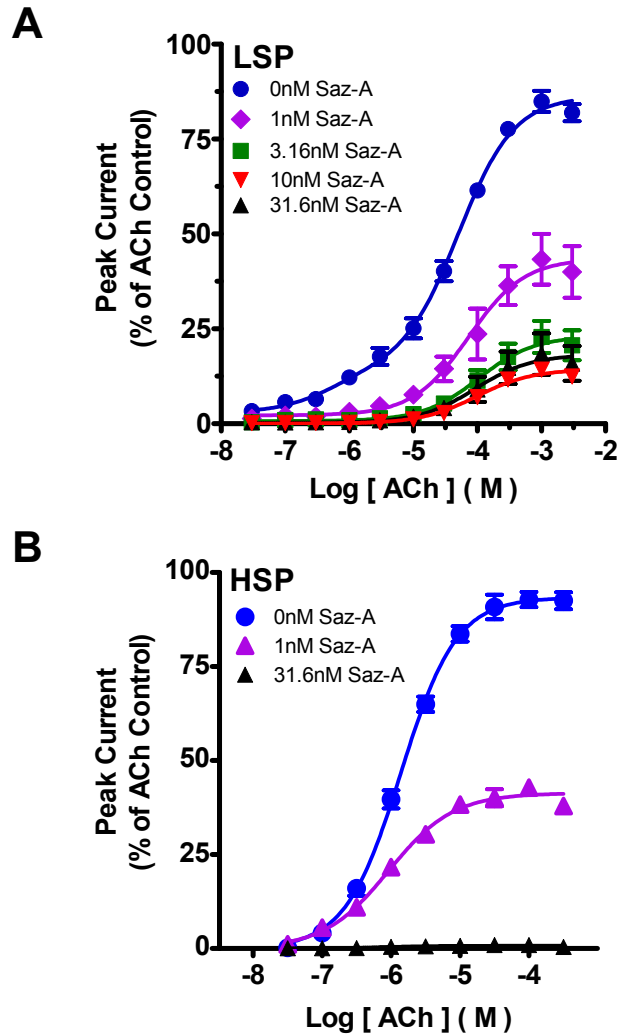


Figure 8

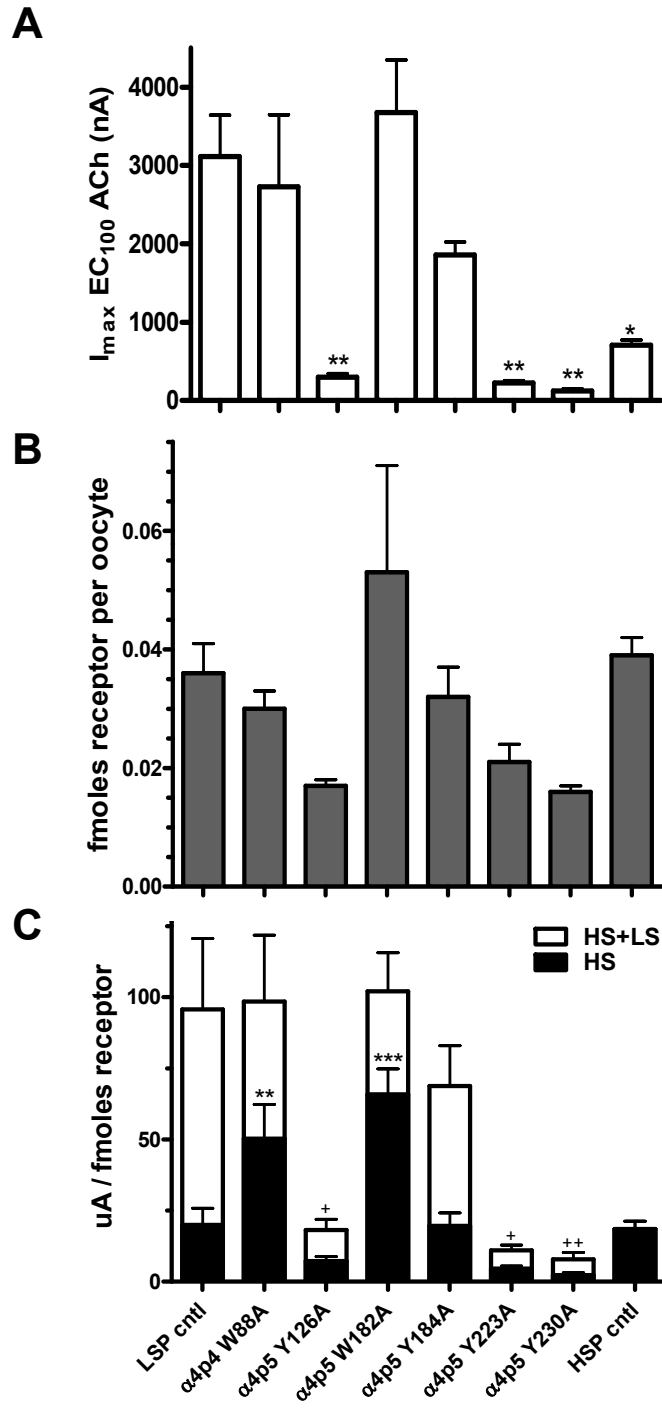


Figure 9

